iScience

CellPress
OPEN ACCESS

Review

Hybprinting for musculoskeletal tissue engineering

Jiannan Li,[1,6] Carolyn Kim,[1,2,6] Chi-Chun Pan,[1,2] Aaron Babian,[3] Elaine Lui,[1,2] Jeffrey L. Young,[1] Seyedsina Moeinzadeh,[1] Sungwoo Kim,[1] and Yunzhi Peter Yang[1,4,5,*]

SUMMARY

This review presents bioprinting methods, biomaterials, and printing strategies that may be used for composite tissue constructs for musculoskeletal applications. The printing methods discussed include those that are suitable for acellular and cellular components, and the biomaterials include soft and rigid components that are suitable for soft and/or hard tissues. We also present strategies that focus on the integration of cell-laden soft and acellular rigid components under a single printing platform. Given the structural and functional complexity of native musculoskeletal tissue, we envision that hybrid bioprinting, referred to as hybprinting, could provide unprecedented potential by combining different materials and bioprinting techniques to engineer and assemble modular tissues.

INTRODUCTION

Addressing musculoskeletal disorders is important because of the vast number of people it impacts as well as the immense financial cost on society. In 2018, the Global Burden of Disease Study identified musculoskeletal disorders as a leading cause of global morbidity (Cottrell and Russell, 2020). Approximately 1.71 billion people have musculoskeletal medical conditions worldwide, and due to the increasing aging population, the number of people with musculoskeletal conditions is projected to increase (Cieza et al., 2021). In the US alone, musculoskeletal diseases cases have greatly increased from 1996 to 2011, with increased cost from $367.1 billion in 1996–1998 to $796.3 billion in 2009–2011 (Yelin et al., 2016).

Native musculoskeletal tissues are challenging to engineer due to their inherent complex mechanical structure and biological composition that often consist of various components including skeletal muscles, bone, tendon, cartilage, vasculature, and the different types of cells that maintain each of these. Skeletal muscles are composed of various types of connective tissues such as perimysium, epimysium, and endomysium, and the muscle fibers themselves are heterogeneous, which add to the challenge of mimicking the structure and function (Ostrovidov et al., 2019). Muscle is connected to bone by tendon, and even this bone-tendon interface—enthesis—is mechanically graded and maintained by multiple musculoskeletal cells that reduce stress concentration and ensure smooth mechanical transfer between bone and soft tissues. Injured zones cannot regenerate the fibrocartilage in enthesis leading to high re-tear rates: surgically re-attached tendons have re-tear rates of 20% for small tears (<3 cm) to 94% for large tears (3–5 cm) (Cheung et al., 2010; Ying et al., 2014). As for vasculature, cells need to be within 100–300 μm from the nearest capillary vessels for effective delivery of oxygen and nutrients and waste removal depending on the metabolic demands of different tissues (Mercado-Pagán et al., 2015). Vascularization is arguably considered the biggest challenge in tissue engineering. Furthermore, nerve fibers and blood vessels course throughout the body in an orderly pattern, often alongside one another (Carmeliet and Tessier-Lavigne, 2005). Reconstructing each individual tissue component is challenging in itself, but engineering a complex functional musculoskeletal tissue with its delicate spatial distribution of bone, cartilage, tendon, muscle, blood vessel, nerve, and skin requires even more sophisticated fabrication techniques.

Recent advances in bioprinting enable fabrication of anatomically shaped tissue engineering constructs with biomimetic complexity and enhanced functionality, albeit with limitations. While great strides have been made via 3D bioprinting to engineer individual musculoskeletal tissue components, no single bioprinting technique can fabricate a functional musculoskeletal implant that can replace or recover the structure and function of damaged or diseased bone and muscle tissues that support locomotion, connect to the vascular network for waste removal and nutrient delivery, and connect to the neuronal network for contraction. We envision hybrid bioprinting, which utilizes multiple printing techniques to support a variety of biomaterials, referred to as hybprinting, can construct such an implant. Combining soft biomaterial

[1]Department of Orthopaedic Surgery, School of Medicine, Stanford University, 300 Pasteur Drive BMI 258, Stanford, CA 94305, USA

[2]Department of Mechanical Engineering, 416 Escondido Mall, Stanford University, Stanford, CA 94305, USA

[3]Department of Biological Sciences, University of California, Davis CA 95616, USA

[4]Department of Materials Science and Engineering, Stanford University, 496 Lomita Mall, Stanford, CA 94305, USA

[5]Department of Bioengineering, Stanford University, 443 Via Ortega, Stanford, CA 94305, USA

[6]These authors contributed equally

*Correspondence: ypyang@stanford.edu

https://doi.org/10.1016/j.isci.2022.104229

Table 1. Resolutions of different printing mechanisms for different applications

Printing mechanisms	Resolutions for different applications		
	Bone	Muscle	Connective tissues
Inkjet printing	0.03–0.085 mm (Cooper et al., 2010; Gao et al., 2015b; Ker et al., 2011; Phillippi et al., 2008; Wang et al., 2021)	0.075 mm (Ker et al., 2011; Phillippi et al., 2008)	0.03–0.127 mm (Cui et al., 2014; Gao et al., 2015b; Ker et al., 2011; Wang et al., 2021)
Stereolithography	0.02–0.05 mm (Lim et al., 2018a; Muralidharan et al., 2019)	0.037 mm (Peele et al., 2015)	0.02–0.05 mm (Lim et al., 2018b; Wang et al., 2015; Zhang et al., 2021b)
Extrusion-based printing	0.1–1.5 mm (Chung et al., 2021; Kajave et al., 2021; Murphy et al., 2017; Romanazzo et al., 2021; Sears et al., 2017)	0.21–0.3 mm (Choi et al., 2019; Laternser et al., 2018)	0.33–0.5 mm (Chae et al., 2021; Laternser et al., 2018; Pati et al., 2014b)
Selective laser sintering	0.04–0.45 mm (Duan et al., 2010; Gayer et al., 2019; Williams et al., 2005; Zhao et al., 2022)	0.1 mm (Yeong et al., 2010)	0.15–0.7 mm (Chen et al., 2011; Garcia-Ruiz and Lantada, 2018; Zheng et al., 2021)
Fused deposition modeling	0.25–0.8 mm (Carlier et al., 2019; Percoco et al., 2020; Wu et al., 2020)	0.4 mm (Rimington et al., 2017)	0.14–0.7 mm (Kwon et al., 2020; Park et al., 2018; Rosenzweig et al., 2015)
Laser-based transfer printing	0.04–0.08 mm (Catros et al., 2011; Keriquel et al., 2017)	0.002–0.3 mm (Ovsianikov et al., 2010; Schiele et al., 2009)	0.04–0.14 mm (Gruene et al., 2011; Koch et al., 2010)
Acoustic droplet ejection	0.01–1 mm (Jentsch et al., 2021)	0.016 mm (Moon et al., 2010)	

printing via stereolithography or extrusion-based printing with rigid biomaterial printing via fused deposition modeling could potentially mimic hybrid bone and muscle/connective tissue grafts. Inkjet printing and acoustic droplet ejection systems could theoretically print graded biochemical cues in precise locations to induce the gradation found in enthesis, which is only 0.1–1 mm in length. Extrusion-based printing is capable of printing cell-laden struts fine enough to be within 100–300 μm as required for vasculature (see Table 1). Existing printing techniques are already being used—most frequently individually as opposed together—to achieve resolutions relevant to musculoskeletal tissue, but there is potential in bringing some of these together for hybprinting (see Table 1). More detailed strategies for hybprinting will be discussed in a later section.

This review describes single printing methods, some commonly used biomaterials, as well as some existing and potential hybprinting strategies that can bypass some of the limitations presented with single printing techniques to print tissue constructs that include the heterogeneous structures, mechanical, and biological gradations, and allow for vasculature. The printing methods include those that are suitable for acellular and cellular components, and the biomaterials include soft and rigid components that are suitable for soft and/or hard tissues. The hybprinting strategies focus on the integration of cell-laden soft and acellular rigid components under a single printing platform. We also propose our envisioned strategies and future directions in hybprinting as more bioprinting mechanisms can be integrated to provide greater potential in musculoskeletal tissue engineering.

MANUFACTURING PROCESSES

Since the 1980s, various 3D printing methods have been developed and commercialized (Elomaa et al., 2015; Elomaa and Yang, 2017). In 2003, Wilson et al. reported one of the first attempts at inkjet-based bioprinting of cells (Wilson and Boland, 2003), after which other attempts at printing cells using extrusion-based and photocrosslinking-based techniques have been applied (Arcaute et al., 2006; Dhariwala et al., 2004; Khalil et al., 2005; Lu et al., 2006; Smith et al., 2004; Wang et al., 2006). Some commonly used techniques are shown in Figure 1 with corresponding tissue engineering applications and resolutions in Table 1: inkjet-based bioprinting (Wilson and Boland, 2003), stereolithography (SLA) (Mondschein et al., 2017), extrusion-based printing (Hoque et al., 2012), selective laser sintering (SLS) (Tan et al., 2005), fused

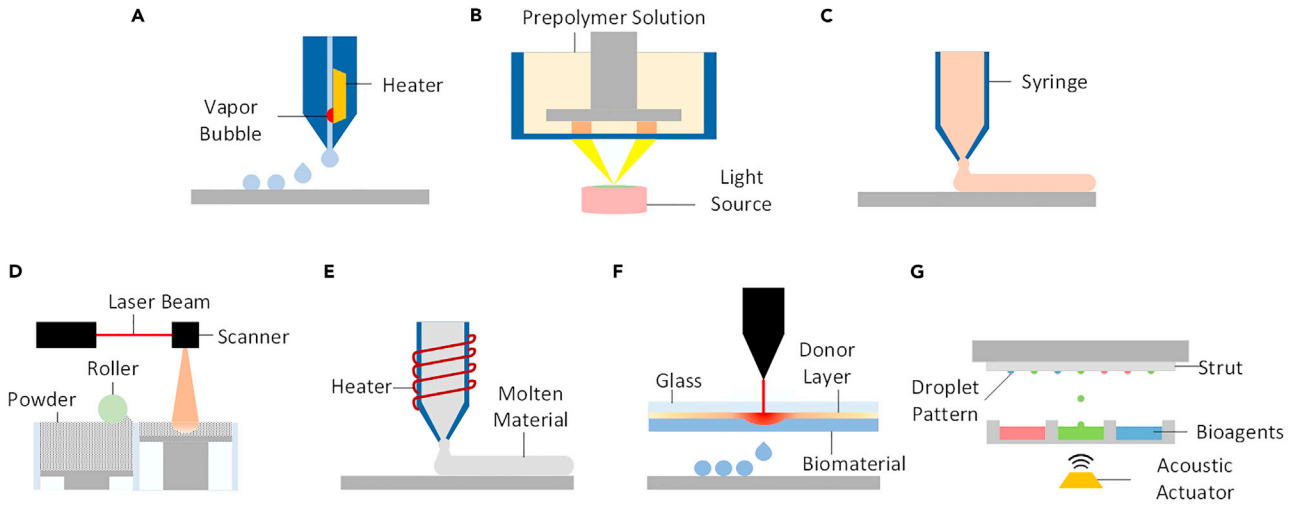

Figure 1. Schematics of 3D printing methods

(A) inkjet-based; (B) stereolithography (SLA); (C) extrusion-based printing; (D) selective laser sintering (SLS); (E) fused deposition modeling (FDM); (F) laser-based transfer printing; (G) acoustic droplet ejection.

deposition modeling (FDM) (Ceretti et al., 2017; Masood et al., 2005; Yen et al., 2009), laser-based transfer bio-printing (Guillemot et al., 2010; Ringeisen et al., 2004), and acoustic droplet ejection (Shanjani et al., 2020).

Inkjet-based bioprinting

Inkjet-based bioprinting is a cell-friendly technique that has been widely used to form 3D constructs by continuously ejecting droplets either with or without cells onto a destination stage using a thermal, piezoelectric, or other actuating mechanism (Figure 1A) (Ding et al., 2015; Graham et al., 2017; Li et al., 2018a, 2018b; Wilson and Boland, 2003; Xu et al., 2013). Each layer is printed by dots, similar to an inkjet paper printer, achieving resolutions <0.1 mm in tissue engineering applications (see Table 1). Gao and company have used this technique to print peptides and human mesenchymal stem cells (hMSCs) to induce osteogenic and chondrogenic differentiation for bone and cartilage formation (Gao et al., 2015b). Ker and company have also inkjet-printed patterns of solid-phase growth factors immobilized onto a substrate to drive muscle-derived stem cells toward osteoblasts on pattern and myoblasts off pattern (Ker et al., 2011). Fast printing speed, compatibility of biological components, and low cost make inkjet-based bioprinters popular for bioprinting applications; however, printhead clogging and material viscosity constraints (Krainer et al., 2019) are often limiting factors with regards to this method.

Stereolithography

SLA is another cell-friendly technique that consists of deflecting a light beam in a horizontal plane to cure a photosensitive material to form a fixed layer within a vat (Elomaa et al., 2015; Mondschein et al., 2017). Each cured layer is then moved along the vertical axis so the next adjoining layer can be cured over it to create a three-dimensional shape, as shown in Figure 1B. This technology permits high-resolution printing with a layer thickness as small as 20 μm and a resolution ranging from 5–300 μm in the horizontal plane (Mondschein et al., 2017). It is worth mentioning that with advanced two-photon lithography or multi-photon lithography techniques, the resolution can be even further improved by three orders of magnitude (Saha et al., 2019; Skylar-Scott et al., 2016). Researchers have used this technique to print constructs that led to bone and cartilage synthesis and even artificial muscle (Lim et al., 2018a; Peele et al., 2015). There are several drawbacks regarding SLA, including cell toxicity due to photo agents and UV, the tradeoff between high resolution and long printing time, and a larger amount of material for the vat, which may be a concern if using expensive and biologically sensitive materials.

Extrusion-based bioprinting

Extrusion-based printing (Hoque et al., 2012) typically utilizes a syringe that is either pneumatic- or piston-driven, and this method can be utilized with cell-laden gels or acellular metal slurries to print rigid scaffolds (Figure 1C). The syringe nozzle follows the desired path layer by layer to fabricate a 3D construct, capable of printing cell-laden struts fine enough to be within 100–300 μm as required to connect to the vascular network (see Table 1). There are derivatives of this printing that include coaxial nozzles or multiple syringe tips to create more complicated designs. For physical hydrogels, the struts are extruded and gelled on the print platform if a physical condition, such as pH or temperature, is changed. Crosslinkable gels can also be used by crosslinking the extruded pre-polymer solution with light or another chemical solution, such as one extruded from a coaxial head or manually added after printing. Feed rates and pressure can be precisely controlled, but a drawback of the syringe printing method is the shear stress that may negatively affect cell viability. As for metal scaffolds, extrusion-based printing has been used to create porous metal scaffolds. The chamber is first filled with metallic slurry and the material is extruded layer by layer, then solidified and sintered (Li et al., 2006).

Selective laser sintering

SLS is based on the movement of a laser source that locally increases the temperature to bind the powder-based material and is typically used for acellular scaffolds (Figure 1D). The laser moves over the powder bed in a layer-by-layer fashion to fabricate a 3D construct (Tan et al., 2005). The resulting construct displays high mechanical strength and complex shapes, as the sintering between layers creates strong bonds and the presence of the un-sintered powder in the bed also provides mechanical support for each layer. Resolution and surface finish vary depending on the type of powder used. When metal is the type of powder used, the method is called selective laser melting (SLM). This process is slightly different, as SLM has the ability to fully melt the metal into a solid 3D construct rather than sinter and fuse the powder together at their points of contact. This technique is used in bone, muscle, and connective tissues, but due to the nature of the types of materials used with SLS, it is most commonly used for bone tissue engineering (see Table 1).

Fused deposition modeling

FDM is one of the most well-known printing methods and consists of an extruding nozzle that follows a designated path in 3D space to deposit strands of molten material (Ceretti et al., 2017; Masood et al., 2005; Yen et al., 2009). The material is heated inside the nozzle and solidifies on either the platform or the previous layer as it gets deposited, as shown in Figure 1E. Owing to this nature, this method is most commonly used for acellular scaffolds as the types of material most suited for the heated extrusion process include polymers and composites. While FDM, like SLS, is also capable of making complex shapes with high strength, overhanging geometries are often more difficult to fabricate as FDM lacks the support that the un-sintered powder bed provides for SLS.

Laser-based transfer bioprinting

Laser-based transfer bioprinting is a method that can be used to transfer cell-laden material from a source plate to a deposition stage by way of using a double-coated source plate, where the donor level absorbs the laser pulse and the heated region generates a bubble that propels a droplet of the material to the stage (Figure 1F) (Guillemot et al., 2010; Ringeisen et al., 2004). This technology bypasses the use of a nozzle, allowing for highly viscous materials to be deposited with high accuracy, unlike inkjet-based bioprinting. One drawback of laser-based transfer bioprinting, however, is the heat generated by the laser that may detrimentally affect cell viability. Researchers have utilized this technique to biofabricate scaffold-free autologous grafts for bone and cartilage and stimulating osteogenesis, among other musculoskeletal tissue engineering applications (Gruene et al., 2011; Ovsianikov et al., 2011).

Acoustic droplet ejection

Another technology that merits mention is acoustic droplet ejection. While this is widely used in high-throughput drug screening, it can be combined with many of the other methods as mentioned previously to add bio-factors in a geometrically controlled manner to create biomimetic constructs in a high-throughput fashion (Shanjani et al., 2020). There are two stages: the destination stage and the source plate (Figure 1G). An acoustic actuator propels the bio-factor from the source plate to the desired location on the destination plate, which may be holding a scaffold, gel, or scaffold-gel hybrid construct. This method can

print droplets onto various layers of the tissue construct and is particularly powerful for creating graded patterns of biological cues. Drawbacks of this method include some residual material left in the source plates, as the acoustic actuator requires a minimum liquid volume to eject droplets accurately.

MATERIALS

Tissue printing for musculoskeletal applications requires both soft and rigid tissue printing. Polymers in hydrogel form can be printed to deliver cells to a desired site, provide space for new tissue formation, or even print soft tissues such as skin. To encapsulate cells, the material must have high water content to allow flow of nutrients and waste, and to provide space for the new tissue, it should also be biodegradable (Lu et al., 2012). Here, we highlight both natural and synthetic polymers that are most commonly used as hydrogels for these soft or hard tissue purposes.

Rigid tissues, such as bone, vary from soft tissues most noticeably in their mechanical strength. Bone is typically classified into two types, trabecular bone or cancellous bone, whose modulus ranges from 2.6–19.4 GPa (Rho et al., 1993, 1997, 1999; Zysset et al., 1999) and cortical bone, where the external cortical bone can have a modulus of anywhere between 14.7–26.6 GPa (DEMPSTER and LIDDICOAT, 1952; Rho et al., 1993; Rho et al., 1999; Rho et al., 1997; Zysset et al., 1999). Load-bearing bone repair involves materials with a comparable mechanical strength or mechanical assistant devices. Soft materials, such as hydrogels, can be used for bone as well, especially with additives or mechanical reinforcement, as summarized in a few excellent review papers (Ashammakhi et al., 2019; Chimene et al., 2016; Chung et al., 2013; Murphy et al., 2013). Here, we will focus on 3D-printed rigid materials with compressive moduli in the range of MPa to GPa for bone applications, including synthetic polymers, metals, and bioceramics. Table 2 presents some recent studies in utilizing different materials for various types of tissues or in conjunction with tissue-specific cells or stem cells. Note that we also summarized the mechanical property range of each material in different applications. However, we only covered the ranges in selected references as it is difficult to be fully comprehensive, and in some applications, the specified material was blended with other materials.

Natural polymeric hydrogels

There are many natural polymeric hydrogels such as agarose, alginate, cellulose, collagen, chitosan, gelatin, fibrinogen/fibrin, and hyaluronic acid (Sabir et al., 2009). While there are studies that explore using these polymers individually, oftentimes researchers create composite gels to take advantage of certain properties of each polymer to improve the overall mechanical or biological properties for tissue engineering. Two of the more commonly used polymers are collagen and alginate.

Collagen is a popular biomaterial for tissue engineering (Baltazar et al., 2020; Du et al., 2015; Jang et al., 2016; Koch et al., 2012; Lee et al., 2009, 2014b; Michael et al., 2013; Min et al., 2018; Skardal et al., 2012), given that it is a natural substrate for multiple cell types, enables cell remodeling, and provides binding sites for cells and growth factors. It is a major structural element of connective tissues, and research has shown that collagen is also a part of many tissues such as bone, ligaments, tendon, dermis, skin, and cartilage. While there are limitations associated with using collagen for tissue engineering applications—such as low modulus, gelation difficulty, and low printing resolutions—researchers have found ways to bypass these issues with a variety of different printing techniques and both chemical and mechanical modifications. Rhee et al. were able to print mechanically stable high-density collagen constructs to support cartilage tissue engineering using a commercial 3D printer (Rhee et al., 2016), and Ren et al. engineered zonal cartilage with a biomimetic chondrocyte density gradient using their custom bioprinter with a 25-gauge needle (Ren et al., 2016).

Alginate is another naturally occurring polymer that is used for soft tissue applications with potential usage for musculoskeletal tissue engineering (Armstrong et al., 2016; Bendtsen et al., 2017; Jang et al., 2016; Luo et al., 2013; Neufurth et al., 2014; Shim et al., 2012; Wust et al., 2014). It is typically obtained from brown seaweed and is commonly used due to its biocompatibility, low toxicity, and mild gelation. While alginate inherently lacks binding sites for cell adhesion and is not degradable in mammals, researchers have found ways to functionalize and engineer alginate and its derivatives to deliver cells and provide space for tissue formation, among other applications (Lee and Mooney, 2012). Moreover, alginate can be printed in a core-shell format with Ca^{2+}, forming fast-curing hollow structure to address vasculature limitations in 3D-printed constructs (Davoodi et al., 2020a). Given its low modulus compared to even soft tissues such as cartilage, which is around 400 kPa, it is often combined with other biomaterials to print bone and cartilage constructs

Table 2. Biomaterials that are suitable for soft and hard tissue bioprinting

Material / Tissue	Compressive modulus	Tensile modulus	Skin	Muscle	Bone	Connective tissue (tendon, ligament, cartilage)	Nerves	Blood vessels
Polymers								
Agarose	20–40 kPa (Lopez-Marcial et al., 2018)	19.2–470 kPa (Guo et al., 2018; Nadernezhad et al., 2019)			(Neufurth et al., 2014)	(Lopez-Marcial et al., 2018)	(Gu et al., 2016)	(Bertassoni et al., 2014b)
Alginate	50–250 kPa (Amr et al., 2021)	9–1132 kPa (Bertuola et al., 2021; Czichy et al., 2020; Heggset et al., 2019; Serafin et al., 2021)		(Chung et al., 2013)	(Armstrong et al., 2016; Bendtsen et al., 2017; Jang et al., 2016; Luo et al., 2013; Neufurth et al., 2014; Shim et al., 2012; Wust et al., 2014)	(Armstrong et al., 2016; Cohen et al., 2010; Gao et al., 2015c; Izadifar et al., 2016; Kundu et al., 2015; Lopez-Marcial et al., 2018; Markstedt et al., 2015; Müller et al., 2017; Shim et al., 2012; Xu et al., 2013; You et al., 2019; Zhang et al., 2013)	(Gu et al., 2016; Hinton et al., 2015; Rajaram et al., 2014)	(Colosi et al., 2016b; Duan et al., 2013; Gao et al., 2019b; Hinton et al., 2015; Kesari et al., 2005; Li et al., 2009; Park et al., 2015; Tabriz et al., 2015; Visser et al., 2013; Xu et al., 2012a; Zhang et al., 2013)
Cellulose	6.3–16.6 MPa (Jiang et al., 2021)	94.6 kPa–152 GPa (Jiang et al., 2021; Li et al., 2019c; Mariani et al., 2019)				(Markstedt et al., 2015; Müller et al., 2017)		
Chitosan	936 Pa–300 kPa (Sadeghianmaryan et al., 2020; Zhang et al., 2018)	3.23–72.12 kPa (Demirtas et al., 2017; Suo et al., 2021; Zhao et al., 2020a)			(Yang et al., 2016b)	(Ye et al., 2014)	(Gu et al., 2016)	(Li et al., 2009; Ulag et al., 2019)
Collagen	0.9 kPa–8.2 MPa (Kajave et al., 2021; Kim and Kim, 2020; Kim et al., 2017; Li et al., 2019b; Rhee et al., 2016; Tirella et al., 2012)	0.654–72.12 kPa (Suo et al., 2021)	(Baltazar et al., 2020; Koch et al., 2012; Lee et al., 2009, 2014b; Michael et al., 2013; Min et al., 2018; Skardal et al., 2012)		(Du et al., 2015; Jang et al., 2016)	(Ren et al., 2016; Rhee et al., 2016; Xu et al., 2013)	(Chen et al., 2018; Lee et al., 2010)	(Chang et al., 2012; Lee et al., 2014a; Park et al., 2015)

(*Continued on next page*)

Table 2. *Continued*

Material / Tissue	Compressive modulus	Tensile modulus	Skin	Muscle	Bone	Connective tissue (tendon, ligament, cartilage)	Nerves	Blood vessels
Fibrinogen/Fibrin	0.058–4 kPa (Duong et al., 2009; Sharma et al., 2021)		(Cubo et al., 2017; Skardal et al., 2012)			(Xu et al., 2013)	(Lee et al., 2010)	(Cui and Boland, 2009; Kolesky et al., 2016; Li et al., 2009)
Gelatin	0.5–250 kPa (Amr et al., 2021; Hsieh and Hsu, 2019)	2.9–534 kPa (Bertuola et al., 2021; Hsieh and Hsu, 2019; Serafin et al., 2021)	(Schiele et al., 2011)	(Chung et al., 2013)	(Neufurth et al., 2014; Wust et al., 2014)			(Colosi et al., 2016b; Duan et al., 2013; Kesari et al., 2005; Kolesky et al., 2016; Lee et al., 2014a; Li et al., 2009; Park et al., 2015)
GelMA	0–320 kPa (Chen et al., 2012; Gao et al., 2019a; Nichol et al., 2010; Schuurman et al., 2013b; Visser et al., 2015b; Zhu et al., 2019)	0–30 kPa (Visser et al., 2015b; Zhu et al., 2019)			(Du et al., 2015; Wenz et al., 2017; Zhou et al., 2016; Zuo et al., 2012)	(Gao et al., 2015a; Grogan et al., 2013; Schuurman et al., 2013a)	(Shin et al., 2012)	(Bertassoni et al., 2014b; Kolesky et al., 2014; Visser et al., 2013)
Hyaluronic acid	1–200 kPa (Choi et al., 2015; Jeon et al., 2007; Seidlits et al., 2010; Tavsanli and Okay, 2017)	0.5–200 kPa (Choi et al., 2015; Jeon et al., 2007; Seidlits et al., 2010; Tavsanli and Okay, 2017)			(Bendtsen et al., 2017; Gao et al., 2014; Wenz et al., 2017)	(Schuurman et al., 2013a)		
PEG/PEGDA/ PEGDMA	0.05–27 MPa (LaNasa et al., 2011; Nguyen et al., 2012; Roberts et al., 2011)	0.016–27 MPa (Hou et al., 2010; LaNasa et al., 2011; Nguyen et al., 2012; Temenoff et al., 2002)	(Rimann et al., 2016)		(Gao et al., 2014; Zuo et al., 2012)	(Cui et al., 2012; Gao et al., 2015a)		(Elomaa et al., 2015; Shanjani et al., 2015)

(*Continued on next page*)

Table 2. *Continued*

Material / Tissue	Compressive modulus	Tensile modulus	Skin	Muscle	Bone	Connective tissue (tendon, ligament, cartilage)	Nerves	Blood vessels
PCL	6.13–161.96 MPa (Olubamiji et al., 2016; Zimmerling et al., 2021)	5.02–1140 MPa (Bruyas et al., 2018; Olubamiji et al., 2016)			(Bruyas et al., 2018, 2019; Jang et al., 2016; Lam et al., 2009; Maruyama et al., 2018; Park et al., 2011; Shim et al., 2012; Shor et al., 2009; Temple et al., 2014)	(Izadifar et al., 2016; Kundu et al., 2015; Shim et al., 2012; Xu et al., 2013)		(Centola et al., 2010; Shanjani et al., 2015; Ulag et al., 2019; Visser et al., 2013)
PLA/PGA/PLGA/ PLLA	0.97–8500 MPa (Dubinenko et al., 2020; Rasoulianboroujeni et al., 2019; Yeo et al., 2021; Zhang et al., 2021c)	112.76 MPa–7.12 GPa (Coppola et al., 2018; Ferreira et al., 2017; Tekinalp et al., 2019)			(Gremare et al., 2018; Kim et al., 2012a; Xu et al., 2019)			(Centola et al., 2010)
PPF		178–199 MPa (Luo et al., 2019a)			(Cooke et al., 2003; Guerra et al., 2019; Kim et al., 2011; Lan et al., 2009; Lee et al., 2006, 2007, 2008, 2011; Luo et al., 2019b; Nettleton et al., 2019; Trachtenberg et al., 2016, 2017)	(Parry et al., 2017)	(Chen et al., 2018)	(Melchiorri et al., 2016; Mishra et al., 2016)
PEEK	0.75–3.4 GPa (Wu et al., 2015; Zanjanijam et al., 2020)	0.1–4.1 GPa (Wu et al., 2015; Yang et al., 2017; Zanjanijam et al., 2020)			(Deng et al., 2017; Feng et al., 2020; Haleem et al., 2019; Han et al., 2019)			
PVA	2.4–960 kPa (Bendtsen et al., 2017; Meng et al., 2020)	1.8–10 MPa (Li et al., 2019a)			(Bendtsen et al., 2017; Wu et al., 2011)			(Visser et al., 2013)

(*Continued on next page*)

Table 2. *Continued*

Material / Tissue	Compressive modulus	Tensile modulus	Skin	Muscle	Bone	Connective tissue (tendon, ligament, cartilage)	Nerves	Blood vessels
Ceramics								
Bioactive glass	0.4–16.5 GPa (Baino and Fiume, 2019; Liu et al., 2013)				(Gao et al., 2014; Luo et al., 2013; Wu et al., 2011)			
BCP	1–40 GPa (Pecqueux et al., 2010; Puertolas et al., 2011)				(Li et al., 2007; Sun et al., 2020)			
Hydroxyapatite	7–13 GPa (Bronzino, 2006)				(Bendtsen et al., 2017; Detsch et al., 2011a; Kim et al., 2012a; Park et al., 2011; Seol et al., 2014; Sun et al., 2020; Trachtenberg et al., 2017; Wenz et al., 2017; Woodard et al., 2007; Wust et al., 2014; Yang et al., 2016a; Zhou et al., 2016)	(You et al., 2019)		
TCP	1–24 GPa (Ajaxon et al., 2017; Qi and Ye, 2009)				(Bruyas et al., 2018, 2019; Butscher et al., 2012; Detsch et al., 2011a; Kalita et al., 2003; Kim et al., 2012a; Lam et al., 2009; Maruyama et al., 2018; Seol et al., 2014; Sun et al., 2020; Tarafder et al., 2013)			

(*Continued on next page*)

Table 2. *Continued*

Material / Tissue	Compressive modulus	Tensile modulus	Skin	Muscle	Bone	Connective tissue (tendon, ligament, cartilage)	Nerves	Blood vessels
Metals								
Co - Cr	2.33–197 GPa (Barazanchi et al., 2020; Han et al., 2017; Limmahakhun et al., 2017)	67–196.2 GPa (Barazanchi et al., 2020; Choi et al., 2014)			(Curodeau et al., 2000; Melican et al., 2001)			
Ti/Ti alloys	0.8–2.4 GPa (Suwanpreecha et al., 2021)	60–105 GPa (Alabort et al., 2022; El-Hajje et al., 2014)			(Dinda et al., 2008; Li et al., 2007; Lopez-Heredia et al., 2008; Tan et al., 2013)			
Mg/Mg alloys	0.2–13.41 GPa (Hong et al., 2016; Li et al., 2021)	38.6–184.4 GPa (Salehi et al., 2019a)			(Salehi et al., 2019a, 2019b)			
Zn/Zn alloys	0.1–13.41 GPa (Cockerill et al., 2020; Salehi et al., 2019a; Wen et al., 2018)	16–32 GPa (Qian et al., 2021)			(Salehi et al., 2019a, 2019b)			
dECM								
dECM				(Choi et al., 2019; Hou et al., 2021; Kim et al., 2020c)	(Chae et al., 2021; Kim et al., 2018b; Nyberg et al., 2017; Wu et al., 2019)	(Chae et al., 2021; Pati et al., 2014a; Toprakhisar et al., 2018; Vernengo et al., 2020; Zhao et al., 2020b, 2021)		

(Hernández-González et al., 2020; Reakasame and Boccaccini, 2018; Sadeghianmaryan et al., 2020). Bendtsen et al. developed an alginate-polyvinyl alcohol-hydroxyapatite hydrogel to bypass the mechanical limitations of alginate alone and successfully demonstrated high cell viability and osteoconductivity in hopes of furthering personalized bone defect treatments (Bendtsen et al., 2017).

Synthetic polymeric hydrogels

There are many types of synthetic polymeric hydrogels such as polyvinyl alcohol (Bendtsen et al., 2017; Wu et al., 2011), polyethylene glycol (Gao et al., 2014; Zuo et al., 2012), and gelatin methacryloyl (GelMA) (Du et al., 2015; Wenz et al., 2017; Zhou et al., 2016; Zuo et al., 2012) that are often used either alone or as a composite polymer blended with either ceramics or other polymers. Compared to natural polymers, synthetic polymers usually provide better tunable mechanical and structural properties, which can easily be controlled by tuning their synthesis process, while also being cell-friendly and relatively inexpensive (Place et al., 2009). Fully synthetic polymers, however, typically lack cell-binding sites or biological cues for desired cell differentiation. Therefore, synthetic soft polymers are frequently used in either cell-free scaffolds or in combination with other components such as gelatin, a collagen derivative, to make a polymer like GelMA for cell attachment and activity.

GelMA is one of the most successful examples of combining synthetic polymers with natural materials. By introducing methacrylate into the linear gelatin polymer, GelMA becomes crosslinkable, allowing the formation of a hydrogel (Klotz et al., 2016). GelMA is soluble at lower temperatures and undergoes gelation below that temperature, and due to its optimal biocompatibility and ease of gelation, it has been widely studied, with concentrated efforts in engineering GelMA into a bioscaffold. Ali Khademhosseini and his group have pioneered the study of using GelMA for tissue engineering (Yue et al., 2015). P. Dubruel et al. have been able to achieve resolutions of 200 μm cell-laden filament sizes (Billiet et al., 2014). Researchers have also used a variety of fabrication techniques such as syringe extrusion (Bertassoni et al., 2014a; Liu et al., 2017) as well as casting the GelMA solution into a 3D-printed sacrificial scaffold, forming a vascularized cell-laden hydrogel (Kolesky et al., 2014). Additives such as nanoparticles or growth factors have also been blended into GelMA hydrogel for specific functions (Du et al., 2015; Xu et al., 2012b). Note that GelMA is a synthetic derivative of gelatin, which is also a frequently used soft natural polymer for bioprinting (Lewis et al., 2018). Gelatin can also be used as sacrificial material due to its ideal melting point (37°C) and has been applied for the formation of vasculature (Noor et al., 2019). It has also been made into microparticles to serve as support bath for extrusion-based printing for the enhancement of print resolution, referred to as the "FRESH" technique, by A. W. Feinberg et al (Hinton et al., 2015). A similar concept, referred to as "SWIFT", was also reported by the J. A. Lewis group using gelatin as a support bath for the fabrication of vascularized tissues (Skylar-Scott et al., 2019b).

Polyethylene glycol (PEG) is another synthetic polymer with great potential. PEG has been widely applied in bioengineering due to its water-soluble and biocompatible properties (Gungor-Ozkerim et al., 2018). By varying its molecular weight and crosslinker, scientists have been able to control the mechanical and viscoelastic properties of PEG and have successfully demonstrated PEG-encapsulated osteoblasts and human MSC viability (Kalakkunnath et al., 2006) (Benoit et al., 2006). Its cytocompatibility can also be improved by tethering to biological molecules such as peptides (Qayyum et al., 2017). PEG-based materials are most commonly used in bioprinting in the form of poly(ethylene glycol) diacrylate (PEGDA) or methacrylate (PEGMA) (Morris et al., 2017), and they are more frequently used in combination with other materials. The combination of PEG-based materials with alginate and GelMA is as aforementioned (Daniele et al., 2014; Gao et al., 2015a; Hockaday et al., 2012; Hong et al., 2015; Mamaghani et al., 2018), where PEG provides mechanical enhancement by reinforcing the hydrogel network. PEG has also been mixed with bioceramics by X. Cui et al. with the addition of hyaluronic acid to encapsulate human MSCs (Gao et al., 2014). In the context of musculoskeletal applications, Gao and company improved properties of bone and cartilage tissue with osteogenic and chondrogenic differentiation of inkjet-printed human MSCs on PEG-GelMA hydrogel scaffolds (Gao et al., 2015a), and Elomaa et al. from our group developed and printed via stereolithography cell-laden biodegradable PEG to engineer preliminary vessel grafts (Elomaa et al., 2015).

Rigid synthetic polymeric scaffolds

Rigid synthetic polymers are used as scaffolds, as their ease of printing allows for controlled pore sizes and unique shapes. There are a number of synthetic polymers that are used in tissue engineering such as

polylactides (Gremare et al., 2018; Kim et al., 2012a; Xu et al., 2019), polycaprolactone (Bruyas et al., 2018, 2019; Jang et al., 2016; Lam et al., 2009; Maruyama et al., 2018; Park et al., 2011; Shim et al., 2012; Shor et al., 2009; Temple et al., 2014), polyether ether ketone (PEEK) (Deng et al., 2017; Feng et al., 2020; Haleem et al., 2019; Han et al., 2019), and poly(propylene fumarate) (PPF) (Cooke et al., 2003; Guerra et al., 2019; Kim et al., 2011; Lan et al., 2009; Lee et al., 2006, 2007, 2008, 2011; Luo et al., 2019b; Nettleton et al., 2019; Trachtenberg et al., 2016, 2017). However, the degradation of synthetic polymers produces acidic by-products that reduce pH and may cause inflammation. To address this, synthetic polymers are often combined with ceramics and natural polymers. For instance, polylactic acid (PLA) is a hydrophobic aliphatic polyester with excellent biocompatibility, thermal stability, and degradation that has been extensively investigated over the last several decades due to its bioresorbable and biocompatible properties (Gremare et al., 2018; Salerno et al., 2015). However, PLA is most frequently studied in combination with other materials, either blended with calcium phosphate or coated by another material, to improve its hydrophilicity and mechanical properties. Additionally, polycaprolactone (PCL) is a semi-crystalline linear resorbable aliphatic polyester that can be used alone but is also typically combined with either alginate to host chondrocytes for hybprinting cartilage tissue (Kundu et al., 2015), beta-tricalcium phosphate (TCP) to augment the Young's modulus and osteoconductivity for bone tissue engineering (Bruyas et al., 2018, 2019; Maruyama et al., 2018), or hydroxyapatite to support cell proliferation and bone cell differentiation also for bone tissue engineering (Park et al., 2011). Combining these synthetic rigid polymers allows for tuning of Young's modulus to make it closer to native tissue, whether that is softer tissues like skin and cartilage (<10 MPa) or spongy bone (200 MPa–5GPa) or harder bone (10–40 GPa) (Alabort et al., 2022; Zhao et al., 2020a). The compressive and tensile moduli ranges are often due to some combination of the base material with other materials that researchers have incorporated.

Metals

Metals have been used for dental and orthopedic applications since the end of the 1960s (Hahn and Palich, 1970; Lueck et al., 1969; Welsh et al., 1971). The most commonly used are titanium, magnesium, zinc, cobalt chromium, and stainless steel. Note that zinc is typically used as a coating or in combination with other polymers or metals (Huang et al., 2016; Place et al., 2011; Swetha et al., 2012; Tripathi et al., 2012; Yusa et al., 2011). Metals possess mechanical properties that are suitable for load-bearing applications, but the mismatch between the Young's modulus of bone (2.6–26.6 GPa) and bulk metallic materials (110 GPa for Ti and 230 GPa for Co-Cr alloys) often leads to stress shielding from the residual bone, which may result in poor fixation of the implant (Tripathi et al., 2012). Recent developments in metallic implant designs, however, focus on adjusting the mechanical properties by applying a porous structure to improve the integration process. Porous metals improve fixation by allowing native bone tissue to grow into and through the metal, bonding the implant to the host bone (Ryan et al., 2006).

Bio-ceramics and bio-glass

Bio-ceramics are considered to be one of the oldest materials used in the human body (Chevalier and Gremillard, 2009). These ceramics include alumina, zirconia (Sakthiabirami et al., 2021a, 2021b), calcium phosphate (CaP) ceramics, and bioactive glass (BG). Ceramics typically come in the form of powders, where traditional fabrication involves cast molding followed by sintering at high temperature (BROUSSAUD, 1989). Because of this, one of the most frequently used 3D printing techniques for bio-ceramics is SLS (Agarwala et al., 1995). SLS was first applied for ceramics fabrication by Lakshminarayan et al (Lakshminarayan and Marcus, 1991; Lakshminarayan et al., 1990). They incorporated a lower-temperature binder considering the high sintering temperature requirement of the bio-ceramics. Despite some disadvantages such as high cost and poor surface finish, SLS is still widely applied for the fabrication of bio-ceramics (Detsch et al., 2011b; Li et al., 2008; Warnke et al., 2010). Other existing 3D printing techniques have also been adopted for manufacturing of bio-ceramics, including SLA, FDM, and inkjet printing. A few reviews have comprehensively covered different 3D printing techniques for ceramics fabrication (Chen et al., 2019; Zafar et al., 2019).

However, with regards to tissue engineering, bio-ceramics and bio-glass can be used to either supplement a material or serve as a base material for bio-printing itself. The addition of bio-ceramics like hydroxyapatite to another base material like PEGDMA is shown to stimulate osteogenesis of printed hMSCs and improve the mechanical properties by increasing the Young's modulus (Gao et al., 2014). Bio-ceramics are sometimes incorporated with metal as well, such as biphasic calcium phosphate ceramic with titanium, to improve the response of bone in the biologically inert metal, resulting in a material that is

osteoconductive and osteoinductive (Li et al., 2007). Bioactive glass has also been explored in tissue engineering due to its excellent bioactivity, degradation, and drug delivery activity. Wu and company printed bioactive glass as the base material with polyvinyl alcohol as a binder with controllable pore architecture and apatite mineralization ability to serve as a candidate for bone regeneration (Wu et al., 2011).

Decellularized extracellular matrix (dECM)

In addition to the various hydrogels developed for tissue engineering, researchers have pursued using deceulluarized extracellular matrix (dECM) as bioinks for 3D printing. While the multiple printing techniques allow for precise location of cells and biochemical cues in the different types of hydrogels and scaffolds carefully tuned to match the mechanical properties of the target tissue, dECM-based bioinks already contain a diverse array of ECM components and conserves native 3D organization, providing necessary cues to the cells for the formation of new tissue. As such, dECM is being used for musculoskeletal tissue regeneration. Chen and company 3D printed electrospun fiber-reinforced dECM, specifically cartilage decellularized matrix, to repair articular cartilage defects in rabbits (Chen et al., 2020). Cho and company 3D printed a tendon-bone interface patch using dECM to accelerate healing in a rat chronic rotator cuff tear model (Chae et al., 2021). Aulino and coworkers demonstrated that dECM scaffolds guide migration and differentiation of stem cells and can be a suitable environment for not only muscle regeneration but also cartilage and bone too (Aulino et al., 2015). Successful utilization of dECM material is a tissue-dependent procedure and residual cellular and nuclear remnants may cause cytotoxicity and immune responses such as inflammation, compromising the benefits of the dECM (Kim et al., 2020a). Overall, the use of dECM has become a whole new paradigm in bioprinting for tissue engineering. Details of using dECM for bioprinting have also been summarized comprehensively in a few well-written review articles (Baiguera et al., 2020; Dzobo et al., 2019; Kim et al., 2018a, 2019). Therefore, we only summarized a few musculoskeletal-related applications for dECM in this review without further expanding the topic (Table 2). Note that the mechanical properties of dECM span too widely across different tissues; hence, they were not included.

HYBPRINTING FOR SOFT-RIGID INTEGRATION

There are a variety of materials and printing technologies to choose from when designing musculoskeletal grafts for bone, cartilage, muscle, or tendon replacement. However, despite numerous discoveries in both soft hydrogel-based scaffolds and rigid polymer-based scaffolds, there is still a technical gap when it comes to the interface between soft-rigid materials. As musculoskeletal grafts are often complex constructs composed of both soft tissues (e.g. muscle, skin, tendon, and cartilage) and rigid tissues (e.g. bone), the demand for engineering such hybrid structures is inevitable. The rigid portion could consist of a combination of natural and synthetic polymers for optimal mechanical properties to provide structural support, enable nutrient and metabolic waste to pass via the pore space, and allow bone tissue ingrowth into the pore space while degrading appropriately. The soft portion could supply the cells and growth factors in geometrically precise areas while also providing space for new tissue formation and more complicated growth, such as cartilage or muscle, in addition to bone. So far, only a few groups have been working on developing hybrid 3D printing techniques, or hybprinting, for the implementation of soft-rigid tissue constructs, with a common strategy of integrating different printing mechanisms in a multi-module platform capable of depositing materials with different properties (Klotz et al., 2016).

As early as 2011, J. Malda et al. started working on the integration of an FDM module with a syringe-based microextrusion (SBM) module to print a rigid PCL scaffold and a soft alginate hydrogel scaffold, yielding the desired mechanical property provided by the PCL scaffold, as well as the proper biocompatibility from the hydrogel scaffold (Figure 2A) (Schuurman et al., 2011). In the same year, D. Cho et al. proposed a similar idea by FDM printing PCL/PLGA and SBM printing hyaluronic acid (HA)/gelatin together (Figure 2B) (Shim et al., 2011). The mechanical properties of the hybrid scaffold as well as cell viability were characterized in these studies. As a result, the mechanical property of the hybrid scaffold is similar to that of the rigid scaffold alone, while achieving high cell viability. In both studies, the hybprinted polymer and hydrogel scaffolds follow a complementary pattern where hydrogel covers the pores of the polymer scaffold. Such design reinforces the hydrogel with the polymer material. Similar designs could also be achieved by simply infusing the polymer scaffold with hydrogel solution followed by crosslinking the hydrogel *in situ* (Boere et al., 2014; Cha et al., 2014; Visser et al., 2015a). In addition to such complementary patterns, A. Atala et al. also investigated layer-by-layer patterns by inkjet printing a cell-laden hydrogel layer followed by electrospinning a polymer layer repeatedly (Xu et al., 2013). Notably, they also built a platform integrating FDM and SBM modules and were able to better mimic human-scale tissue by introducing a

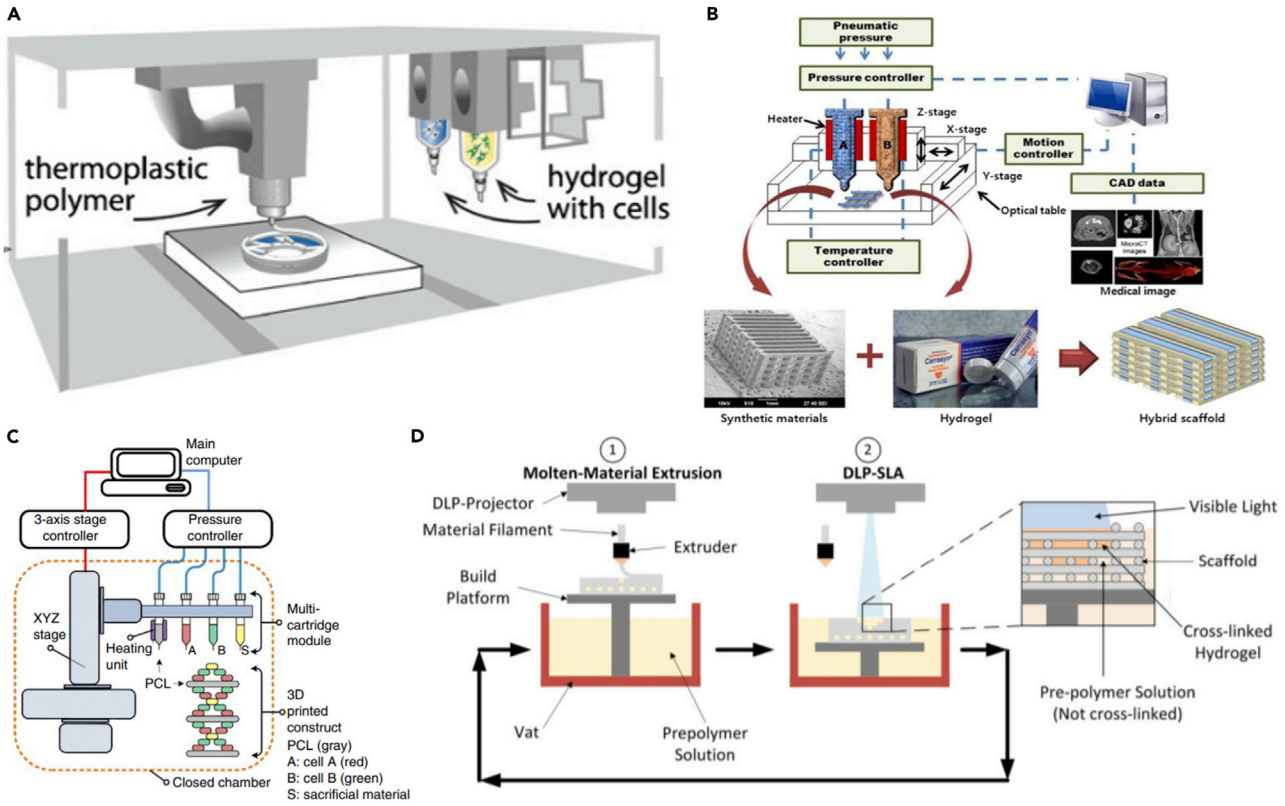

Figure 2. Recent progress in hybprinting for soft-rigid scaffolds integration

(A–C) Integration of FDM with SBM module by (A) (J) Malda (Schuurman et al., 2011), (B) (D) Cho (Shim et al., 2011), and (C) (A) Atala group (Kang et al., 2016). (D) Integration of FDM with SLA by Y.P. Yang group (Shanjani et al., 2015). (Reproduced with the permission from (A, B, D) IOP Publishing and (C) Springer Nature).

sacrificial material for more complicated patterns (Figure 2C) (Kang et al., 2016). Specifically, they printed PCL/TCP scaffolds with FDM for structural support, and gelatin/fibrinogen/HA/glycerol hydrogel with SBM for cell encapsulation, and Pluronic F127 with SBM as the sacrificial material. Various cell types, including bone, cartilage, and skeletal muscle cells, were encapsulated for the engineering of complex physiological relevant tissue scaffolds. Over the past decade, these groups continued in the hybprinting direction for various applications including bone (Shim et al., 2012), tendon (Chae et al., 2021), cartilage regeneration (Galarraga et al., 2021; Kundu et al., 2015; Schuurman et al., 2013a; Visser et al., 2013), and other applications (Cho et al., 2021; Kim et al., 2021). Specifically, D. Cho and coworkers have been focusing on developing various decellularized ECM for multiple tissue engineering applications (Cho et al., 2021), notably bone-tendon interface (Chae et al., 2021). Moreover, J. Malda and coworkers also systematically studied and reviewed the underlying structural, mechanical, and chemical properties of multi-tissue or multi-material interfaces, which provide insight for engineering a multi-tissue construct (Viola et al., 2021). A few other groups also joined the effort in developing integrated 3D printing systems for complex tissues engineering (Daly et al., 2016; Izadifar et al., 2016; Lee et al., 2013; Rak Kwon et al., 2020; Touré et al., 2020; Zhang et al., 2021a). In these works, PCL and alginate/GelMA/HA are the most frequently used as base materials for rigid polymer and soft hydrogel scaffolds, respectively, while other components could be added for specific purposes, such as bioactive glass for enhancing mechanical property and inducing bone or tendon development (Touré et al., 2020). Notably, S. Lee and coworkers have hybprinted an MSC-laden PCL/HA scaffold for the improvement of enthesis regeneration in a full-thickness rabbit rotator cuff tear model. These advancements show that hybprinting techniques have potential in future clinical translation. Thus far, the integration efforts mainly focus on FDM and SBM modules, as they are the most commonly applied bioprinting techniques for these materials. Digital light processing stereolithography (DLP-SLA) has been a widely applied 3D printing technique in the manufacturing industry as well as bioengineering (Li et al., 2020). In 2015, our group introduced a hybrid bioprinting platform, referred to as Hybprinter, by combining

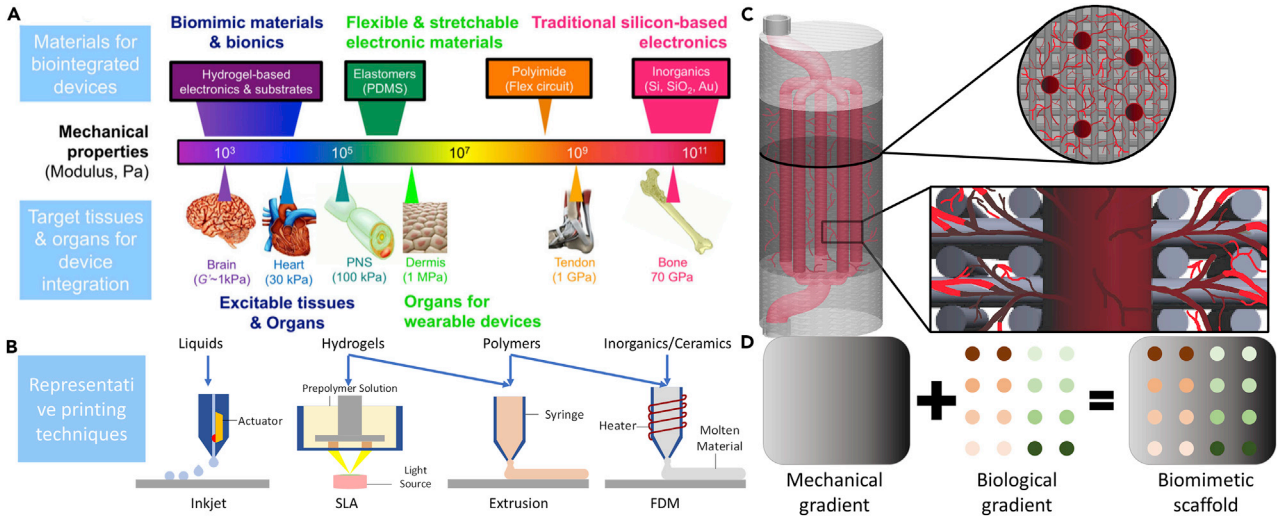

Figure 3. Hybprinting logistics and envisioned strategies for musculoskeletal tissue engineering

(A) Mechanical property range of different tissues and materials (Bettinger, 2018); (B) Corresponding printing mechanisms for each engineered materials; (C) Schematic of hybprinted vascularized musculoskeletal construct. The grey lattice indicates the bone scaffold printed by FDM, the red conduit indicates the major vascular branches by DLP-SLA, and the space between the grey lattice and red conduits are for the cell-laden hydrogel for angiogenesis and osteogenesis by SBM. (D) By incorporating other printing mechanisms such as inkjet printing, we envision the fabrication of more biomimetic tissue constructs by combining the mechanical gradient and biological gradient. (Reproduced with the permission from (A) Springer Nature).

DLP-SLA and FDM (Shanjani et al., 2015). The schematic of Hybprinter is shown in Figure 2D. As a demonstration, PCL and PEGDA were hybprinted with the FDM and DLP-SLA modules, respectively. This was the first time SLA was integrated with FDM for the fabrication of soft-rigid tissue interfaces. Seamless integration can be achieved with high resolution facilitated by the SLA module. Moreover, given the advantage of SLA printing, hollow structures mimicking blood vessels were able to be directly printed. We were also able to encapsulate human umbilical vein endothelial cells (HUVEC) in the printed structure with high viability for the formation of vessels during a perfusion study (Kim et al., 2020b).

Another possibility for soft-rigid integration, in addition to hybprinting, would be casting a porous bioresorbable rigid scaffold with soft polymers that provide additional bioactive materials to encourage bone ingrowth (de Moraes et al., 2012; Gong et al., 2007; Kim et al., 2012b; Melchels et al., 2012; Mintz and Cooper, 2014; Santos et al., 2008; Schuurman et al., 2011; Shanjani et al., 2017; Temple et al., 2014). Research reports thus far suggest that a combination of biomaterials, whether through material blends, coatings, or hybrid printing, must be used to enhance load-bearing bone formation, as no single material is capable of providing a mechanically robust bone substitute while encouraging osteogenesis and vascularization.

FUTURE DIRECTIONS AND ENVISIONED STRATEGIES FOR MUSCULOSKELETAL TISSUE ENGINEERING WITH HYBPRINTING

It can be seen that other than our group's integration of FDM and SLA, current efforts in hybprinting mainly focus on integrating FDM and SBM. This is possibly because these two modules are the most widely used printing techniques and because they share a similar mechanism, which is to extrude the material, either heated or non-heated, through an orifice. Therefore, the integration of these two modules is considered relatively straightforward. However, we believe the future of hybprinting will require the integration of several different printing modules for the fabrication of more sophisticated tissue constructs. Particularly, the mechanical and biological property of different tissues is so distinct, as their mechanical properties span over 8 orders of magnitude (Figure 3A) (Bettinger, 2018). While different biomaterials have been developed for specific tissues with certain properties, they usually only work with a specific type of printing technology (Figure 3B). As each printing module possesses different advantages and disadvantages, a more comprehensive platform would be able to utilize the advantage of each module to improve the overall print quality and maximize tissue construct functionality. For example, in previous works, researchers have already started integrating more than one SBM modules into a single platform (Kang et al., 2016;

Schuurman et al., 2011). This allows for SBM printing of tissue-specific bioinks incorporating different cells, gel compositions, or growth factors. In this way, each bioink can be tailored and optimized to target tissue in a multi-tissue engineering process. In our previous work (Shanjani et al., 2015), by introducing DLP-SLA, we were able to achieve more complicated structures, taking advantage of the high resolution provided by SLA. Taking one step further, future work may include the integration of these three printing modules, including FDM, SLA, and SBM into one platform. Based on such envisioned platform, we propose future strategies for engineering musculoskeletal tissue constructs, including printing vascularized bone tissue scaffolds by dedicating DLP-SLA for complex vascular branches, FDM for rigid bone structural support, and SBM for cell-laden hydrogels for osteogenesis and angiogenesis (Figure 3C). Note that multiple FDM and SBM printheads could also be implemented for multiple tissue purposes. Specifically, angiogenesis could be achieved by incorporating different growth factors into the hydrogel bioink for guided sprouting of microvasculature. We have proven this can be done in a recent study with a GelMA/PEGDMA dual hydrogel system (Kim et al., 2020b). Also, different modules of Hybprinter can be used for different functions. For example, SBM can be used to fabricate blood vessels, and DLP-SLA can be used to photocrosslink the printed hydrogel structures to enhance the mechanical properties and structural integrity of such complex structures. Such a combinatory platform offers the potential to fabricate constructs at multi-order magnitudes with a large range of mechanical and rheological properties to match soft-hard tissue mechanical interfaces, as well as to control the placement of biological materials, such as growth factors and cell types, to encourage biomimetic cell differentiation and growth.

Moreover, we envision that introducing other printing mechanisms will further expand the capability of the hybprinting platform. For example, laser-based printing techniques, including SLS or laser-based transfer printing, are commonly used with ceramic materials, and therefore may be incorporated to enforce the rigid scaffold. Additionally, inkjet or ADE printing can precisely control minute amounts of liquid solutions, and therefore may be used to pattern chemical or biological reagents onto the scaffolds. The addition of inkjet or ADE printing has great potential to reproduce the biochemical cues found in the native human body. With an inkjet or ADE printing module, one could precisely control the location and quantity of the bioreagents in an aqueous format, generating the desired biological gradient in the engineered scaffold. Combined with the previously achieved mechanical gradient by the integration of FDM, SLA, and SBM, we can engineer a more biomimetic tissue scaffold for musculoskeletal applications (Figure 3D). A more specific example could be applying droplet dispensing for various growth factor (GF) patterns on the hybrid scaffold envisioned in Figure 3C, where bone and angiogenesis inducing GFs can be deposited onto corresponding locations. This method combines FDM for structural support and bone inducing scaffold, SLA for cell encapsulation and major vessel formation, and droplet dispensing for GF patterning. The incorporation of different modules will be able to cover a much wider range of viscosities, resolutions, and mechanical properties to address multi-tissue complexity. In our envisioned approach, the bone scaffold and major vessels would be hybprinted first, followed by GF-induced angiogenesis to form microvasculature, leading to a fully functional large bone graft. Thus far, inkjet or ADE printing has yet to be reported to have been integrated with other 3D printing mechanisms, with the exception of electrospinning (Xu et al., 2013). In addition to these integrations, we anticipate other integrations and breakthroughs in the future of hybprinting to create a new era for musculoskeletal tissue engineering.

In addition to the printing modules in Figure 1, other printing modules may be incorporated into hybprinting, as well as other tissue engineering techniques to supplement hybprinting. As briefly mentioned above, electrospinning, in some ways similar to extrusion bioprinting, could be combined to form hybrid scaffolds (Xu et al., 2013). Microfluidics also sheds light on fabricating multi-material, graded scaffolds (Colosi et al., 2016a; Davoodi et al., 2020b; Skylar-Scott et al., 2019a). Moreover, external mechanical stimuli also play an important role in musculoskeletal tissue development (Nordberg et al., 2018). To study these effects, bioreactors have been fabricated and used to mechanically condition engineered scaffolds (Todros et al., 2021). Also important to note, the interface of a multi-tissue hybrid scaffold is often the weakest point and potentially becomes a breakpoint under mechanical stress, requiring special treatment such as chemical reinforcement to strengthen the interface. In sum, much more is yet to be explored for hybprinting, which cannot be comprehensively covered in this review.

CONCLUSION

We have reviewed different printing mechanisms, as well as commonly used materials for tissue engineering applications. For engineering complex musculoskeletal tissues, we envision that integration of multiple

printing mechanism will have great potential due to its ability to handle multiple materials. Although human printing has long been envisioned by science fiction and even Hollywood, in reality, we still have a long way to go. Along with the fabrication and biomaterial challenges described above, there are a few fundamental challenges in hybprinting vascularized composite tissue constructs for musculoskeletal tissue engineering. First, it will be difficult to incorporate neurovascular bundle or beds into the printed constructs to form vascularized, innervated bone, muscle, and skin tissues as modular tissue or tissue "Legos." The second challenge would be seamlessly integrating vascularized, innervated bone, muscle, and skin tissues and maturing the composite tissue construct into a functional musculoskeletal graft. In other words, the difficulty lies in assembling these modular tissues, or tissue "Legos," and maturing the tissue assembly into a functional composite tissue construct. Thirdly, sterilizing the hybprinted tissues and safely transporting them between the manufacturing facility and operation room would be difficult. Lastly, we must successfully engraft the hybprinted tissue into patients with large traumas and diseases to restore functionality while minimizing side effects such as immune rejection. The key factor that determines the engraftment success of the engineered graft depends on the integration of the graft and host, which occurs on multiple levels, such as vascularization, innervation, structure, etc. If integration is not successful in any of one of these levels, the treatment will potentially fail or be delayed. Without vascularization, the tissues will not grow into the scaffold; without innervation, there will be a lack of control or acceleration in the formation of functional tissue; and without structural connection, the scaffold will not be stable. As such, integration between the engineered construct and the host is crucial for functional restoration and true regeneration.

In combination with advanced bioreactor technologies, hybprinting attempts to address the first and second challenges by integrating advanced additive manufacturing, robotics, biofactors, stem cells, and biomaterials. Hybprinting simultaneously provides new tools and strategies for modeling tissue response and engineering biomimetic composite tissue constructs with embedded vasculatures and nerve bundles for musculosketal tissue engineering. Even though the field of bioprinting has advanced greatly in recent years, the field is still in its infancy and needs further research with particular attention on optimizing the materials and designs for fabrication and maturation of functional composite tissue constructs and regulatory pathways for clinical applications.

ACKNOWLEDGMENTS

This research was funded through the financial support of NIAMS grants U01AR069395, R01AR072613, R01AR074458, DoD grants W81XWH-20-1-0343 and W81XWH-21-PR211291, the Stanford Woods Institute for the Environments, Boswell Foundation, Tad and Diane Taube Family Foundation, and Stanford Maternal & Child Health Research Institute postdoc fellowship.

AUTHOR CONTRIBUTIONS

J.L., C.K., and YP.Y. conceived and performed investigation. J.L., C.K., A.B., and YP.Y wrote the manuscript. E.L., C.P, JL.Y., S.M., and S.K. supervised, reviewed, and edited the manuscript. YP.Y. secured the funding.

DECLARATION OF INTERESTS

The authors declare no competing interests.

REFERENCES

Agarwala, M., Bourell, D., Beaman, J., Marcus, H., and Barlow, J. (1995). Direct selective laser sintering of metals. Rapid Prototyping J. *1*, 26–36. https://doi.org/10.1108/13552549510078113.

Ajaxon, I., Acciaioli, A., Lionello, G., Ginebra, M.P., Ohman-Magi, C., Baleani, M., and Persson, C. (2017). Elastic properties and strain-to-crack-initiation of calcium phosphate bone cements: revelations of a high-resolution measurement technique. J. Mech. Behav. Biomed. *74*, 428–437. https://doi.org/10.1016/j.jmbbm.2017.06.023.

Alabort, W., Tang, Y.T., Barba, D., and Reed, R.C. (2022). Alloys-by-design: a low-modulus titanium alloy for additively manufactured biomedical implants. Acta Materialia *229*, 117749.

Amr, M., Dykes, I., Counts, M., Kernan, J., Mallah, A., Mendenhall, J., Van Wie, B., Abu-Lail, N., and Gozen, A. (2021). 3D printed, mechanically tunable, composite sodium alginate, gelatin and Gum Arabic (SA-GEL-GA) scaffolds. Bioprinting *22*, e00133.

Arcaute, K., Mann, B., and Wicker, R. (2006). Stereolithography of three-dimensional bioactive poly(ethylene glycol) constructs with encapsulated cells. Ann. Biomed. Eng. *34*, 1429–1441. https://doi.org/10.1007/s10439-006-9156-y.

Armstrong, J.P., Burke, M., Carter, B.M., Davis, S.A., and Perriman, A.W. (2016). 3D bioprinting using a templated porous bioink. Adv. Healthc. Mater. *5*, 1724–1730. https://doi.org/10.1002/adhm.201600022.

Ashammakhi, N., Hasan, A., Kaarela, O., Byambaa, B., Sheikhi, A., Gaharwar, A., and Khademhosseini, A. (2019). Advancing frontiers in bone bioprinting. Advanced healthcare materials. UNSP *8*, 1801048. https://doi.org/10.1002/adhm.201801048.

Aulino, P., Costa, A., Chiaravalloti, E., Perniconi, B., Adamo, S., Coletti, D., Marrelli, M., Tatullo, M., and Teodori, L. (2015). Muscle xtracellular matrix scaffold is a multipotent environment. Int. J. Med. Sci. *12*, 336–340. https://doi.org/10.7150/ijms.10761.

Baiguera, S., Del Gaudio, C., Di Nardo, P., Manzari, V., Carotenuto, F., and Teodori, L. (2020). 3D printing decellularized extracellular matrix to design biomimetic scaffolds for skeletal muscle tissue engineering. Biomed. Res. Int. *2020*, 2689701. https://doi.org/10.1155/2020/2689701.

Baino, F., and Fiume, E. (2019). Elastic mechanical properties of 45S5-based bioactive glass-ceramic scaffolds. Materials *12*, 3244. https://doi.org/10.3390/ma12193244.

Baltazar, T., Merola, J., Catarino, C., Xie, C., Kirkiles-Smith, N., Lee, V., Hotta, S., Dai, G., Xu, X., Ferreira, F., et al. (2020). Three dimensional bioprinting of a vascularized and perfusable skin graft using human keratinocytes, fibroblasts, pericytes, and endothelial cells. Tissue Eng. A *26*, 227–238. https://doi.org/10.1089/ten.tea.2019.0201.

Barazanchi, A., Li, K., Al-Amleh, B., Lyons, K., and Waddell, J. (2020). Mechanical properties of laser-sintered 3D-printed cobalt chromium and soft-milled cobalt chromium. Prosthesis *2*. https://doi.org/10.3390/prosthesis2040028.

Bendtsen, S., Quinnell, S., and Wei, M. (2017). Development of a novel alginate-polyvinyl alcohol-hydroxyapatite hydrogel for 3D bioprinting bone tissue engineered scaffolds. J. Biomed. Mater. Res. A *105*, 1457–1468. https://doi.org/10.1002/jbm.a.36036.

Benoit, D., Durney, A., and Anseth, K. (2006). Manipulations in hydrogel degradation behavior enhance osteoblast function and mineralized tissue formation. Tissue Eng. *12*, 1663–1673. https://doi.org/10.1089/ten.2006.12.1663.

Bertassoni, L., Cardoso, J., Manoharan, V., Cristino, A., Bhise, N., Araujo, W., Zorlutuna, P., Vrana, N., Ghaemmaghami, A., Dokmeci, M., and Khademhosseini, A. (2014a). Direct-write bioprinting of cell-laden methacrylated gelatin hydrogels. Biofabrication *6*, 024105. https://doi.org/10.1088/1758-5082/6/2/024105.

Bertassoni, L., Cecconi, M., Manoharan, V., Nikkhah, M., Hjortnaes, J., Cristino, A., Barabaschi, G., Demarchi, D., Dokmeci, M., Yang, Y., and Khademhosseini, A. (2014b). Hydrogel bioprinted microchannel networks for vascularization of tissue engineering constructs. Lab A Chip *14*, 2202–2211. https://doi.org/10.1039/c4lc00030g.

Bertuola, M., Araoz, B., Gilabert, U., Gonzalez-Wusener, A., Perez-Recalde, M., Arregui, C., and Hermida, E. (2021). Gelatin-alginate-hyaluronic acid inks for 3D printing: effects of bioglass addition on printability, rheology and scaffold tensile modulus. J. Mater. Sci. *56*, 15327–15343. https://doi.org/10.1007/s10853-021-06250-0.

Bettinger, C.J. (2018). Recent advances in materials and flexible electronics for peripheral nerve interfaces. Bioelectron. Med. *4*, 6. https://doi.org/10.1186/s42234-018-0007-6.

Billiet, T., Gevaert, E., De Schryver, T., Cornelissen, M., and Dubruel, P. (2014). The 3D printing of gelatin methacrylamide cell-laden tissue-engineered constructs with high cell viability. Biomaterials *35*, 49–62. https://doi.org/10.1016/j.biomaterials.2013.09.078.

Boere, K., Visser, J., Seyednejad, H., Rahimian, S., Gawlitta, D., van Steenbergen, M., Dhert, W., Hennink, W., Vermonden, T., and Malda, J. (2014). Covalent attachment of a three-dimensionally printed thermoplast to a gelatin hydrogel for mechanically enhanced cartilage constructs. Acta Biomater. *10*, 2602–2611. https://doi.org/10.1016/j.actbio.2014.02.041.

Bronzino, J.D. (2006). The Biomedical Engineering Handbook, 3 Edition (CRC Press Taylor & Francis Group).

BROUSSAUD, D. (1989). Engineering ceramics. Mater. Sci. Eng. a-Structural Mater. Properties Microstructure Process. *109*, 335. https://doi.org/10.1016/0921-5093(89)90611-4.

Bruyas, A., Lou, F., Stahl, A., Gardner, M., Maloney, W., Goodman, S., and Yang, Y. (2018). Systematic characterization of 3D-printed PCL/beta-TCP scaffolds for biomedical devices and bone tissue engineering: influence of composition and porosity. J. Mater. Res. *33*, 1948–1959. https://doi.org/10.1557/jmr.2018.112.

Bruyas, A., Moeinzadeh, S., Kim, S., Lowenberg, D., and Yang, Y. (2019). Effect of electron beam sterilization on three-dimensional-printed polycaprolactone/beta-tricalcium phosphate scaffolds for bone tissue engineering. Tissue Eng. Part a *25*, 248–256. https://doi.org/10.1089/ten.tea.2018.0130.

Butscher, A., Bohner, M., Roth, C., Ernstberger, A., Heuberger, R., Doebelin, N., von Rohr, P., and Muller, R. (2012). Printability of calcium phosphate powders for three-dimensional printing of tissue engineering scaffolds. Acta Biomater. *8*, 373–385. https://doi.org/10.1016/j.actbio.2011.08.027.

Carlier, E., Marquette, S., Peerboom, C., Denis, L., Benali, S., Raquez, J.M., Amighi, K., and Goole, J. (2019). Investigation of the parameters used in fused deposition modeling of poly (lactic acid) to optimize 3D printing sessions. Int. J. Pharmaceutics *565*, 367–377. https://doi.org/10.1016/j.ijpharm.2019.05.008.

Carmeliet, P., and Tessier-Lavigne, M. (2005). Common mechanisms of nerve and blood vessel wiring. Nature *436*, 193–200. https://doi.org/10.1038/nature03875.

Catros, S., Fricain, J.C., Guillotin, B., Pippenger, B., Bareille, R., Remy, M., Lebraud, E., Desbat, B., Amedee, J., and Guillemot, F. (2011). Laser-assisted bioprinting for creating on-demand patterns of human osteoprogenitor cells and nano-hydroxyapatite. Biofabrication *3*, 025001. https://doi.org/10.1088/1758-5082/3/2/025001.

Centola, M., Rainer, A., Spadaccio, C., De Porcellinis, S., Genovese, J.A., and Trombetta, M. (2010). Combining electrospinning and fused deposition modeling for the fabrication of a hybrid vascular graft. Biofabrication *2*, 014102. https://doi.org/10.1088/1758-5082/2/1/014102.

Ceretti, E., Ginestra, P., Neto, P., Fiorentino, A., Da Silva, J., Shih, A., and Cao, J. (2017). Multi-layered scaffolds production via Fused Deposition Modeling (FDM) using an open source 3D printer: process parameters optimization for dimensional accuracy and design reproducibility. 3rd Cirp Conf. Biomanufacturing *65*, 13–18. https://doi.org/10.1016/j.procir.2017.04.042.

Cha, C., Soman, P., Zhu, W., Nikkhah, M., Camci-Unal, G., Chen, S., and Khademhosseini, A. (2014). Structural reinforcement of cell-laden hydrogels with microfabricated three dimensional scaffolds. Biomater. Sci. *2*, 703–709. https://doi.org/10.1039/c3bm60210a.

Chae, S., Sun, Y., Choi, Y.J., Ha, D.H., Jeon, I.H., and Cho, D.W. (2021). 3D cell-printing of tendon-bone interface using tissue-derived extracellular matrix bioinks for chronic rotator cuff repair. Biofabrication *13*, 035005. https://doi.org/10.1088/1758-5090/abd159.

Chang, C., Krishnan, L., Nunes, S., Church, K., Edgar, L., Boland, E., Weiss, J., Williams, S., and Hoying, J. (2012). Determinants of microvascular network topologies in implanted neovasculatures. Arteriosclerosis Thromb. Vasc. Biol. *32*, 5–U55. https://doi.org/10.1161/ATVBAHA.111.238725.

Chen, C.H., Chen, J.P., and Lee, M.Y. (2011). Effects of gelatin modification on rapid prototyping pcl scaffolds for cartilage engineering. J. Mech. Med. Biol. *11*, 993–1002. https://doi.org/10.1142/S0219519411004848.

Chen, W., Xu, Y., Li, Y., Jia, L., Mo, X., Jiang, G., and Zhou, G. (2020). 3D printing electrospinning fiber-reinforced decellularized extracellular matrix for cartilage regeneration. Chem. Eng. J *382*, 122986. https://doi.org/10.1016/j.cej.2019.122986.

Chen, X., Zhao, Y., Li, X., Xiao, Z., Yao, Y., Chu, Y., Farkas, B., Romano, I., Brandi, F., and Dai, J. (2018). Functional multichannel poly(propylene fumarate)-collagen scaffold with collagen-binding neurotrophic factor 3 promotes neural regeneration after transected spinal cord injury. Adv. Healthc. Mater *7*, 1800315. https://doi.org/10.1002/adhm.201800315.

Chen, Y.C., Lin, R.Z., Qi, H., Yang, Y., Bae, H., Melero-Martin, J.M., and Khademhosseini, A. (2012). Functional human vascular network generated in photocrosslinkable gelatin methacrylate hydrogels. Adv. Funct. Mater. *22*, 2027–2039. https://doi.org/10.1002/adfm.201101662.

Chen, Z., Li, Z., Li, J., Liu, C., Lao, C., Fu, Y., Liu, C., Li, Y., Wang, P., and He, Y. (2019). 3D printing of ceramics: a review. J. Eur. Ceram. Soc. *39*, 661–687. https://doi.org/10.1016/j.jeurceramsoc.2018.11.013.

Cheung, E.V., Silverio, L., and Sperling, J.W. (2010). Strategies in biologic augmentation of rotator cuff repair: a review. Clin. Orthop. Relat. Res. *468*, 1476–1484. https://doi.org/10.1007/s11999-010-1323-7.

Chevalier, J., and Gremillard, L. (2009). Ceramics for medical applications: a picture for the next 20 years. J. Eur. Ceram. Soc. *29*, 1245–1255. https://doi.org/10.1016/j.jeurceramsoc.2008.08.025.

Chimene, D., Lennox, K.K., Kaunas, R.R., and Gaharwar, A.K. (2016). Advanced bioinks for 3D printing: a materials science perspective. Ann. Biomed. Eng. *44*, 2090–2102. https://doi.org/10.1007/s10439-016-1638-y.

Cho, W.W., Kim, B.S., Ahn, M., Ryu, Y.H., Ha, D.H., Kong, J.S., Rhie, J.W., and Cho, D.W. (2021). Flexible adipose-vascular tissue assembly using combinational 3D printing for volume-stable soft

tissue reconstruction. Adv. Healthc. Mater *10*, e2001693. https://doi.org/10.1002/adhm.202001693.

Choi, S.C., Yoo, M.A., Lee, S.Y., Lee, H.J., Son, D.H., Jung, J., Noh, I., and Kim, C.W. (2015). Modulation of biomechanical properties of hyaluronic acid hydrogels by crosslinking agents. J. Biomed. Mater. Res. A *103*, 3072–3080. https://doi.org/10.1002/jbm.a.35437.

Choi, Y.-J., Koak, J.-Y., Heo, S.-J., Kim, S.-K., Ahn, J.-S., and Park, D.-S. (2014). Comparisons of the mechanical properties and microstructures of fractured surface for Co-Cr alloy fabricated by conventional cast, 3-D printing laser-sintered and CAD/CAM milled techniques. J. Korean Acad. Prosthodont. *52*, 67–73.

Choi, Y.J., Jun, Y.J., Kim, D.Y., Yi, H.G., Chae, S.H., Kang, J., Lee, J., Gao, G., Kong, J.S., Jang, J., et al. (2019). A 3D cell printed muscle construct with tissue-derived bioink for the treatment of volumetric muscle loss. Biomaterials *206*, 160–169. https://doi.org/10.1016/j.biomaterials.2019.03.036.

Chung, J., Naficy, S., Yue, Z., Kapsa, R., Quigley, A., Moulton, S., and Wallace, G. (2013). Bio-ink properties and printability for extrusion printing living cells. Biomater. Sci. *1*, 763–773. https://doi.org/10.1039/c3bm00012e.

Chung, J.J., Yoo, J., Sum, B.S.T., Li, S.W., Lee, S., Kim, T.H., Li, Z.L., Stevens, M.M., Georgiou, T.K., Jung, Y., and Jones, J.R. (2021). 3D printed porous methacrylate/silica hybrid scaffold for bone substitution. Adv. Healthc. Mater *10*, 2100117. https://doi.org/10.1002/adhm.202100117.

Cieza, A., Causey, K., Kamenov, K., Hanson, S.W., Chatterji, S., and Vos, T. (2021). Global estimates of the need for rehabilitation based on the global burden of disease study 2019: a systematic analysis for the global burden of disease study 2019. Lancet *396*, 2006–2017. https://doi.org/10.1016/S0140-6736(20)32340-0.

Cockerill, I., Su, Y., Sinha, S., Qin, Y., Zheng, Y., Young, M., and Zhu, D. (2020). Porous zinc scaffolds for bone tissue engineering applications: a novel additive manufacturing and casting approach. Mater. Sci. Eng. C-Materials Biol. Appl *110*, 110738. https://doi.org/10.1016/j.msec.2020.110738.

Cohen, D., Lipton, J., Bonassar, L., and Lipson, H. (2010). Additive manufacturing for in situ repair of osteochondral defects. Biofabrication *2*, 035004. https://doi.org/10.1088/1758-5082/2/3/035004.

Colosi, C., Shin, S.R., Manoharan, V., Massa, S., Costantini, M., Barbetta, A., Dokmeci, M.R., Dentini, M., and Khademhosseini, A. (2016a). Microfl uidic bioprinting of heterogeneous 3D tissue constructs using low-viscosity bioink. Adv. Mater. *28*, 677–684. https://doi.org/10.1002/adma.201503310.

Colosi, C., Shin, S.R., Manoharan, V., Massa, S., Costantini, M., Barbetta, A., Dokmeci, M.R., Dentini, M., and Khademhosseini, A. (2016b). Microfluidic bioprinting of heterogeneous 3D tissue constructs using low-viscosity bioink. Adv. Mater. *28*, 677–684. https://doi.org/10.1002/adma.201503310.

Cooke, M., Fisher, J., Dean, D., Rimnac, C., and Mikos, A. (2003). Use of stereolithography to manufacture critical-sized 3D biodegradable scaffolds for bone ingrowth. J. Biomed. Mater. Res. B-Applied Biomater. *64B*, 65–69. https://doi.org/10.1002/jbm.b.10485.

Cooper, G.M., Miller, E.D., DeCesare, G.E., Usas, A., Lensie, E.L., Bykowski, M.R., Huard, J., Weiss, L.E., Losee, J.E., and Campbell, P.G. (2010). Inkjet-based biopatterning of bone morphogenetic protein-2 to spatially control calvarial bone formation. Tissue Eng. A *16*, 1749–1759. https://doi.org/10.1089/ten.tea.2009.0650.

Coppola, B., Cappetti, N., Di Maio, L., Scarfato, P., and Incarnato, L. (2018). 3D printing of PLA/clay nanocomposites: influence of printing temperature on printed samples properties. Materials *11*, 1947. https://doi.org/10.3390/ma11101947.

Cottrell, M., and Russell, T. (2020). Telehealth for musculoskeletal physiotherapy. Musculoskelet. Sci. Practice *48*, 102193. https://doi.org/10.1016/j.msksp.2020.102193.

Cubo, N., Garcia, M., del Canizo, J., Velasco, D., and Jorcano, J. (2017). 3D bioprinting of functional human skin: production and in vivo analysis. Biofabrication *9*, 015006. https://doi.org/10.1088/1758-5090/9/1/015006.

Cui, X., and Boland, T. (2009). Human microvasculature fabrication using thermal inkjet printing technology. Biomaterials *30*, 6221–6227. https://doi.org/10.1016/j.biomaterials.2009.07.056.

Cui, X., Breitenkamp, K., Finn, M.G., Lotz, M., and D'Lima, D.D. (2012). Direct human cartilage repair using three-dimensional bioprinting technology. Tissue Eng. Part A. *18*, 1304–1312. https://doi.org/10.1089/ten.TEA.2011.0543.

Cui, X.F., Gao, G.F., Yonezawa, T., and Dai, G.H. (2014). Human cartilage tissue fabrication using three-dimensional inkjet printing technology. Jove-j Vis. Exp, e51294. https://doi.org/10.3791/51294.

Curodeau, A., Sachs, E., and Caldarise, S. (2000). Design and fabrication of cast orthopedic implants with freeform surface textures from 3-D printed ceramic shell. J. Biomed. Mater. Res. *53*, 525–535. https://doi.org/10.1002/1097-4636(200009)53:5<525::AID-JBM12>3.0.CO;2-1.

Czichy, C., Spangenberg, J., Gunther, S., Gelinsky, M., and Odenbach, S. (2020). Determination of the Young's modulus for alginate-based hydrogel with magnetite-particles depending on storage conditions and particle concentration. J. Magnetism Magn. Mater *501*, 166395. https://doi.org/10.1016/j.jmmm.2020.166395.

Daly, A., Cunniffe, G., Sathy, B., Jeon, O., Alsberg, E., and Kelly, D. (2016). 3D bioprinting of developmentally inspired templates for whole bone organ engineering. Adv. Healthc. Mater. *5*, 2353–2362. https://doi.org/10.1002/adhm.201600182.

Daniele, M., Adams, A., Naciri, J., North, S., and Ligler, F. (2014). Interpenetrating networks based on gelatin methacrylamide and PEG formed using concurrent thiol click chemistries for hydrogel tissue engineering scaffolds. Biomaterials *35*, 1845–1856. https://doi.org/10.1016/j.biomaterials.2013.11.009.

Davoodi, E., Sarikhani, E., Montazerian, H., Ahadian, S., Costantini, M., Swieszkowski, W., Willerth, S., Walus, K., Mofidfar, M., Toyserkani, E., et al. (2020a). Extrusion and microfluidic-based bioprinting to fabricate biomimetic tissues and organs. Adv. Mater. Technol. *5*. https://doi.org/10.1002/admt.201901044.

Davoodi, E., Sarikhani, E., Montazerian, H., Ahadian, S., Costantini, M., Swieszkowski, W., Willerth, S.M., Walus, K., Mofidfar, M., Toyserkani, E., et al. (2020b). Extrusion and microfluidic-based bioprinting to fabricate biomimetic tissues and organs. Adv. Mater. Technol-us *5*, 1901044. https://doi.org/10.1002/admt.201901044.

de Moraes, M., Paternotte, E., Mantovani, D., and Beppu, M. (2012). Mechanical and biological performances of new scaffolds made of collagen hydrogels and fibroin microfibers for vascular tissue engineering. Macromolecular Biosci. *12*, 1253–1264. https://doi.org/10.1002/mabi.201200060.

Demirtas, T., Irmak, G., and Gumusderelioglu, M. (2017). A bioprintable form of chitosan hydrogel for bone tissue engineering. Biofabrication *9*, 035003. https://doi.org/10.1088/1758-5090/aa7b1d.

DEMPSTER, W., and LIDDICOAT, R. (1952). Compact bone as a NON-isotropic material. Am. J. Anat. *91*, 331–362. https://doi.org/10.1002/aja.1000910302.

Deng, L., Deng, Y., and Xie, K. (2017). AgNPs-decorated 3D printed PEEK implant for infection control and bone repair. Colloids Surf. B-Biointerfaces *160*, 483–492. https://doi.org/10.1016/j.colsurfb.2017.09.061.

Detsch, R., Schaefer, S., Deisinger, U., Ziegler, G., Seitz, H., and Leukers, B. (2011a). In vitro-osteoclastic activity studies on surfaces of 3D printed calcium phosphate scaffolds. J. Biomater. Appl. *26*, 359–380. https://doi.org/10.1177/0885328210373285.

Detsch, R., Schaefer, S., Deisinger, U., Ziegler, G., Seitz, H., and Leukers, B. (2011b). In vitro: osteoclastic activity studies on surfaces of 3D printed calcium phosphate scaffolds. J. Biomater. Appl. *26*, 359–380. https://doi.org/10.1177/0885328210373285.

Dhariwala, B., Hunt, E., and Boland, T. (2004). Rapid prototyping of tissue-engineering constructs, using photopolymerizable hydrogels and stereolithography. Tissue Eng. *10*, 1316–1322. https://doi.org/10.1089/1076327042500256.

Dinda, G., Song, L., and Mazumder, J. (2008). Fabrication of Ti-6Al-4V scaffolds by direct metal deposition. Metallurgical Mater. Trans. a-Physical Metall. Mater. Sci. *39A*, 2914–2922. https://doi.org/10.1007/s11661-008-9634-y.

Ding, Y.Z., Li, J.N., Xiao, W.W., Xiao, K., Lee, J., Bhardwaj, U., Zhu, Z.J., Digiglio, P., Yang, G.M., Lam, K.S., and Pan, T.R. (2015). Microfluidic-enabled print-to-screen platform for high-throughput screening of combinatorial chemotherapy. Anal. Chem. *87*, 10166–10171. https://doi.org/10.1021/acs.analchem.5b00826.

Du, M., Chen, B., Meng, Q., Liu, S., Zheng, X., Zhang, C., Wang, H., Li, H., Wang, N., and Dai, J. (2015). 3D bioprinting of BMSC-laden methacrylamide gelatin scaffolds with CBD-BMP2-collagen microfibers. Biofabrication *7*, 044104. https://doi.org/10.1088/1758-5090/7/4/044104.

Duan, B., Hockaday, L., Kang, K., and Butcher, J. (2013). 3D Bioprinting of heterogeneous aortic valve conduits with alginate/gelatin hydrogels. J. Biomed. Mater. Res. Part a *101*, 1255–1264. https://doi.org/10.1002/jbm.a.34420.

Duan, B., Wang, M., Zhou, W.Y., Cheung, W.L., Li, Z.Y., and Lu, W.W. (2010). Three-dimensional nanocomposite scaffolds fabricated via selective laser sintering for bone tissue engineering. Acta Biomater. *6*, 4495–4505. https://doi.org/10.1016/j.actbio.2010.06.024.

Dubinenko, G., Zinoviev, A., Bolbasov, E., Novikov, V., and Tverdokhlebov, S. (2020). Preparation of Poly(L-lactic acid)/Hydroxyapatite composite scaffolds by fused deposit modeling 3D printing. Mater. Today-Proceedings *22*, 228–234.

Duong, H., Wu, B., and Tawil, B. (2009). Modulation of 3D fibrin matrix stiffness by intrinsic fibrinogen-thrombin compositions and by extrinsic cellular activity. Tissue Eng. Part a *15*, 1865–1876. https://doi.org/10.1089/ten.tea.2008.0319.

Dzobo, K., Motaung, K., and Adesida, A. (2019). Recent trends in decellularized extracellular matrix bioinks for 3D printing: an updated review. Int. J. Mol. Sci. *20*. https://doi.org/10.3390/ijms20184628.

El-Hajje, A., Kolos, E., Wang, J., Maleksaeedi, S., He, Z., Wiria, F., Choong, C., and Ruys, A. (2014). Physical and mechanical characterisation of 3D-printed porous titanium for biomedical applications. J. Mater. Science-Materials Med. *25*, 2471–2480. https://doi.org/10.1007/s10856-014-5277-2.

Elomaa, L., Pan, C.C., Shanjani, Y., Malkovskiy, A., Seppälä, J.V., and Yang, Y. (2015). Three-dimensional fabrication of cell-laden biodegradable poly(ethylene glycol-. J. Mater. Chem. B *3*, 8348–8358. https://doi.org/10.1039/c5tb01468a.

Elomaa, L., and Yang, Y.P. (2017). Additive manufacturing of vascular grafts and vascularized tissue constructs. Tissue Eng. Part B Rev. *23*, 436–450. https://doi.org/10.1089/ten.TEB.2016.0348.

Feng, P., Jia, J., Peng, S., Yang, W., Bin, S., and Shuai, C. (2020). Graphene oxide-driven interfacial coupling in laser 3D printed PEEK/PVA scaffolds for bone regeneration. Virtual Phys. Prototyping *15*, 211–226. https://doi.org/10.1080/17452759.2020.1719457.

Ferreira, R., Amatte, I., Dutra, T., and Burger, D. (2017). Experimental characterization and micrography of 3D printed PLA and PLA reinforced with short carbon fibers. Composites B-Engineering *124*, 88–100. https://doi.org/10.1016/j.compositesb.2017.05.013.

Galarraga, J.H., Locke, R.C., Witherel, C.E., Stoeckl, B.D., Castilho, M., Mauck, R.L., Malda, J., Levato, R., and Burdick, J.A. (2021). Fabrication of MSC-laden composites of hyaluronic acid hydrogels reinforced with MEW scaffolds for cartilage repair. Biofabrication *14*. https://doi.org/10.1088/1758-5090/ac3acb.

Gao, F., Xu, Z., Liang, Q., Li, H., Peng, L., Wu, M., Zhao, X., Cui, X., Ruan, C., and Liu, W. (2019a). Osteochondral regeneration with 3D-printed biodegradable high-strength supramolecular polymer reinforced-gelatin hydrogel scaffolds. Adv. Sci. (Weinh) *6*, 1900867. https://doi.org/10.1002/advs.201900867.

Gao, G., Kim, H., Kim, B., Kong, J., Lee, J., Park, B., Chae, S., Kim, J., Ban, K., Jang, J., et al. (2019b). Tissue-engineering of vascular grafts containing endothelium and smooth-muscle using triple-coaxial cell printing. Appl. Phys. Rev *6*, 041402. https://doi.org/10.1063/1.5099306.

Gao, G., Schilling, A., Hubbell, K., Yonezawa, T., Truong, D., Hong, Y., Dai, G., and Cui, X. (2015a). Improved properties of bone and cartilage tissue from 3D inkjet-bioprinted human mesenchymal stem cells by simultaneous deposition and photocrosslinking in PEG-GelMA. Biotechnol. Lett. *37*, 2349–2355. https://doi.org/10.1007/s10529-015-1921-2.

Gao, G., Schilling, A., Yonezawa, T., Wang, J., Dai, G., and Cui, X. (2014). Bioactive nanoparticles stimulate bone tissue formation in bioprinted three-dimensional scaffold and human mesenchymal stem cells. Biotechnol. J. *9*, 1304–1311. https://doi.org/10.1002/biot.201400305.

Gao, G.F., Yonezawa, T., Hubbell, K., Dai, G.H., and Cui, X.F. (2015b). Inkjet-bioprinted acrylated peptides and PEG hydrogel with human mesenchymal stem cells promote robust bone and cartilage formation with minimal printhead clogging. Biotechnol. J. *10*, 1568–1577. https://doi.org/10.1002/biot.201400635.

Gao, Q., He, Y., Fu, J., Liu, A., and Ma, L. (2015c). Coaxial nozzle-assisted 3D bioprinting with built-in microchannels for nutrients delivery. Biomaterials *61*, 203–215. https://doi.org/10.1016/j.biomaterials.2015.05.031.

Garcia-Ruiz, J.P., and Lantada, A.D. (2018). 3D printed structures filled with carbon fibers and functionalized with mesenchymal stem cell conditioned media as in vitro cell niches for promoting chondrogenesis. Materials *11*, 23. https://doi.org/10.3390/ma11010023.

Gayer, C., Ritter, J., Bullemer, M., Grom, S., Jauer, L., Meiners, W., Pfister, A., Reinauer, F., Vucak, M., Wissenbach, K., et al. (2019). Development of a solvent-free polylactide/calcium carbonate composite for selective laser sintering of bone tissue engineering scaffolds. Mater. Sci. Eng. C-Materials Biol. Appl. *101*, 660–673. https://doi.org/10.1016/j.msec.2019.03.101.

Gong, Y., He, L., Li, J., Zhou, Q., Ma, Z., Gao, C., and Shen, J. (2007). Hydrogel-filled polylactide porous scaffolds for cartilage tissue engineering. J. Biomed. Mater. Res. B Appl. Biomater. *82*, 192–204. https://doi.org/10.1002/jbm.b.30721.

Graham, A.D., Olof, S.N., Burke, M.J., Armstrong, J.P.K., Mikhailova, E.A., Nicholson, J.G., Box, S.J., Szele, F.G., Perriman, A.W., and Bayley, H. (2017). High-resolution patterned cellular constructs by droplet-based 3D printing. Sci. Rep. *7*, 7004. https://doi.org/10.1038/s41598-017-06358-x.

Gremare, A., Guduric, V., Bareille, R., Heroguez, V., Latour, S., L'heureux, N., Fricain, J., Catros, S., and Le Nihouannen, D. (2018). Characterization of printed PLA scaffolds for bone tissue engineering. J. Biomed. Mater. Res. Part a *106*, 887–894. https://doi.org/10.1002/jbm.a.36289.

Grogan, S., Chung, P., Soman, P., Chen, P., Lotz, M., Chen, S., and D'Lima, D. (2013). Digital micromirror device projection printing system for meniscus tissue engineering. Acta Biomater. *9*, 7218–7226. https://doi.org/10.1016/j.actbio.2013.03.020.

Gruene, M., Deiwick, A., Koch, L., Schlie, S., Unger, C., Hofmann, N., Bernemann, I., Glasmacher, B., and Chichkov, B. (2011). Laser printing of stem cells for biofabrication of scaffold-free autologous grafts. Tissue Eng. C-Methods *17*, 79–87. https://doi.org/10.1089/ten.tec.2010.0359.

Gu, Q., Tomaskovic-Crook, E., Lozano, R., Chen, Y., Kapsa, R., Zhou, Q., Wallace, G., and Crook, J. (2016). Functional 3D neural mini-tissues from printed gel-based bioink and human neural stem cells. Adv. Healthc. Mater. *5*, 1429–1438. https://doi.org/10.1002/adhm.201600095.

Guerra, A., Lammel-Lindemann, J., Katko, A., Kleinfehn, A., Rodriguez, C., Catalani, L., Becker, M., Ciurana, J., and Dean, D. (2019). Optimization of photocrosslinkable resin components and 3D printing process parameters. Acta Biomater. *97*, 154–161. https://doi.org/10.1016/j.actbio.2019.07.045.

Guillemot, F., Souquet, A., Catros, S., Guillotin, B., Lopez, J., Faucon, M., Pippenger, B., Bareille, R., Remy, M., Bellance, S., et al. (2010). High-throughput laser printing of cells and biomaterials for tissue engineering. Acta Biomater. *6*, 2494–2500. https://doi.org/10.1016/j.actbio.2009.09.029.

Gungor-Ozkerim, P.S., Inci, I., Zhang, Y.S., Khademhosseini, A., and Dokmeci, M.R. (2018). Bioinks for 3D bioprinting: an overview. Biomater. Sci. *6*, 915–946. https://doi.org/10.1039/c7bm00765e.

Guo, J., Zhang, R., Zhang, L., and Cao, X. (2018). 4D printing of robust hydrogels consisted of agarose nanofibers and polyacrylamide. Acs Macro Lett. *7*, 442–446. https://doi.org/10.1021/acsmacrolett.7b00957.

Hahn, H., and Palich, W. (1970). Preliminary evaluation of porous metal surfaced titanium for orthopedic implants. J. Biomed. Mater. Res. *4*, 571–577. https://doi.org/10.1002/jbm.820040407.

Haleem, A., Javaid, M., Vaish, A., and Vaishya, R. (2019). Three-dimensional-printed polyether ether ketone implants for orthopedics. Indian J. Orthop. *53*, 377–379. https://doi.org/10.4103/ortho.IJOrtho_499_18.

Han, C., Yao, Y., Cheng, X., Luo, J., Luo, P., Wang, Q., Yang, F., Wei, Q., and Zhang, Z. (2017). Electrophoretic deposition of gentamicin-loaded silk fibroin coatings on 3D-printed porous cobalt-chromium-molybdenum bone substitutes to prevent orthopedic implant infections. Biomacromolecules *18*, 3776–3787. https://doi.org/10.1021/acs.biomac.7b01091.

Han, X., Sharma, N., Xu, Z., Scheideler, L., Geis-Gerstorfer, J., Rupp, F., Thieringer, F., and Spintzyk, S. (2019). An in vitro study of osteoblast response on fused-filament fabrication 3D printed PEEK for dental and cranio-maxillofacial implants. J. Clin. Med *8*, 771. https://doi.org/10.3390/jcm8060771.

Heggset, E., Strand, B., Sundby, K., Simon, S., Chinga-Carrasco, G., and Syverud, K. (2019). Viscoelastic properties of nanocellulose based inks for 3D printing and mechanical properties of CNF/alginate biocomposite gels. Cellulose *26*, 581–595. https://doi.org/10.1007/s10570-018-2142-3.

Hernández-González, A.C., Téllez-Jurado, L., and Rodríguez-Lorenzo, L.M. (2020). Alginate hydrogels for bone tissue engineering, from injectables to bioprinting: a review. Carbohydr. Polym. *229*, 115514. https://doi.org/10.1016/j.carbpol.2019.115514.

Hinton, T., Jallerat, Q., Palchesko, R., Park, J., Grodzicki, M., Shue, H., Ramadan, M., Hudson, A., and Feinberg, A. (2015). Three-dimensional printing of complex biological structures by freeform reversible embedding of suspended hydrogels. Sci. Adv. *1*. https://doi.org/10.1126/sciadv.1500758.

Hockaday, L., Kang, K., Colangelo, N., Cheung, P., Duan, B., Malone, E., Wu, J., Girardi, L., Bonassar, L., Lipson, H., et al. (2012). Rapid 3D printing of anatomically accurate and mechanically heterogeneous aortic valve hydrogel scaffolds. Biofabrication *4*, 035005. https://doi.org/10.1088/1758-5082/4/3/035005.

Hong, D., Chou, D., Velikokhatnyi, O., Roy, A., Lee, B., Swink, I., Issaev, I., Kuhn, H., and Kumta, P. (2016). Binder-jetting 3D printing and alloy development of new biodegradable Fe-Mn-Ca/Mg alloys. Acta Biomater. *45*, 375–386. https://doi.org/10.1016/j.actbio.2016.08.032.

Hong, S., Sycks, D., Chan, H., Lin, S., Lopez, G., Guilak, F., Leong, K., and Zhao, X. (2015). 3D printing of highly stretchable and tough hydrogels into complex, cellularized structures. Adv. Mater. *27*, 4035–4040. https://doi.org/10.1002/adma.201501099.

Hoque, M.E., Chuan, Y.L., and Pashby, I. (2012). Extrusion based rapid prototyping technique: an advanced platform for tissue engineering scaffold fabrication. Biopolymers *97*, 83–93. https://doi.org/10.1002/bip.21701.

Hou, C.X., Zheng, J.H., Li, Z.K., Qi, X.J., Tian, Y.P., Zhang, M.L., Zhang, J.K., and Huang, X.H. (2021). Printing 3D vagina tissue analogues with vagina decellularized extracellular matrix bioink. Int. J. Biol. Macromolecules *180*, 177–186. https://doi.org/10.1016/j.ijbiomac.2021.03.070.

Hou, Y., Schoener, C.A., Regan, K.R., Munoz-Pinto, D., Hahn, M.S., and Grunlan, M.A. (2010). Photo-cross-linked PDMSstar-PEG hydrogels: synthesis, characterization, and potential application for tissue engineering scaffolds. Biomacromolecules *11*, 648–656. https://doi.org/10.1021/bm9012293.

Hsieh, C., and Hsu, S. (2019). Double-network polyurethane-gelatin hydrogel with tunable modulus for high-resolution 3D bioprinting. Acs Appl. Mater. Inter. *11*, 32746–32757. https://doi.org/10.1021/acsami.9b10784.

Huang, Y., Zhang, X., Qiao, H., Hao, M., Zhang, H., Xu, Z., Zhang, X., Pang, X., and Lin, H. (2016). Corrosion resistance and cytocompatibility studies of zinc-doped fluorohydroxyapatite nanocomposite coatings on titanium implant. Ceramics Int. *42*, 1903–1915. https://doi.org/10.1016/j.ceramint.2015.09.160.

Izadifar, Z., Chang, T., Kulyk, W., Chen, X., and Eames, B. (2016). Analyzing biological performance of 3D-printed, cell-impregnated hybrid constructs for cartilage tissue engineering. Tissue Eng. Part C-Methods *22*, 173–188. https://doi.org/10.1089/ten.tec.2015.0307.

Jang, C., Ahn, S., Yang, G., and Kim, G. (2016). A MSCs-laden polycaprolactone/collagen scaffold for bone tissue regeneration. Rsc Adv. *6*, 6259–6265. https://doi.org/10.1039/c5ra20627h.

Jentsch, S., Nasehi, R., Kuckelkorn, C., Gundert, B., Aveic, S., and Fischer, H. (2021). Multiscale 3D bioprinting by nozzle-free acoustic droplet ejection. Small Methods *5*, 2000971. https://doi.org/10.1002/smtd.202000971.

Jeon, O., Song, S.J., Lee, K.J., Park, M.H., Lee, S.H., Hahn, S.K., Kim, S., and Kim, B.S. (2007). Mechanical properties and degradation behaviors of hyaluronic acid hydrogels cross-linked at various cross-linking densities. Carbohyd Polym. *70*, 251–257. https://doi.org/10.1016/j.carbpol.2007.04.002.

Jiang, J., Oguzlu, H., and Jiang, F. (2021). 3D printing of lightweight, super-strong yet fl exible all-cellulose structure. Chem. Eng. J *405*, 126668. https://doi.org/10.1016/j.cej.2020.126668.

Kajave, N.S., Schmitt, T., Nguyen, T.U., Gaharwar, A.K., and Kishore, V. (2021). Bioglass incorporated methacrylated collagen bioactive ink for 3D printing of bone tissue. Biomed. Mater *16*, 035003. https://doi.org/10.1088/1748-605X/abc744.

Kalakkunnath, S., Kalika, D., Lin, H., and Freeman, B. (2006). Viscoelastic characteristics of UV polymerized poly(ethylene glycol) diacrylate networks with varying extents of crosslinking. J. Polym. Sci. B-Polymer Phys. *44*, 2058–2070. https://doi.org/10.1002/polb.20873.

Kalita, S., Bose, S., Hosick, H., and Bandyopadhyay, A. (2003). Development of controlled porosity polymer-ceramic composite scaffolds via fused deposition modeling. Mater. Sci. Eng. C-Biomimetic Supramolecular Syst. *23*, 611–620. https://doi.org/10.1016/S0928-4931(03)00052-3.

Kang, H., Lee, S., Ko, I., Kengla, C., Yoo, J., and Atala, A. (2016). A 3D bioprinting system to produce human-scale tissue constructs with structural integrity. Nat. Biotechnol. *34*, 312. https://doi.org/10.1038/nbt.3413.

Ker, E.D.F., Chu, B., Phillippi, J.A., Gharaibeh, B., Huard, J., Weiss, L.E., and Campbell, P.G. (2011). Engineering spatial control of multiple differentiation fates within a stem cell population. Biomaterials *32*, 3413–3422. https://doi.org/10.1016/j.biomaterials.2011.01.036.

Keriquel, V., Oliveira, H., Remy, M., Ziane, S., Delmond, S., Rousseau, B., Rey, S., Catros, S., Amedee, J., Guillemot, F., and Fricain, J.C. (2017). In situ printing of mesenchymal stromal cells, by laser-assisted bioprinting, for in vivo bone regeneration applications. Scientific Reports *7*, 1778. https://doi.org/10.1038/s41598-017-01914-x.

Kesari, P., Xu, T., Boland, T., Laurencin, C., and Botchwey, E. (2005). Layer-by-layer printing of cells and its application to tissue engineering. Nanoscale Mater. Sci. Biol. Med. *845*, 111–117.

Khalil, S., Nam, J., and Sun, W. (2005). Multi-nozzle deposition for construction of 3D biopolymer tissue scaffolds. Rapid Prototyping J. *11*, 9–17. https://doi.org/10.1108/13552540510573347.

Kim, B., Das, S., Jang, J., and Cho, D. (2020a). Decellularized extracellular matrix-based bioinks for engineering tissue- and organ-specific microenvironments. Chem. Rev. *120*, 10941–10994. https://doi.org/10.1021/acs.chemrev.9b00808.

Kim, B.S., Ahn, M., Cho, W.W., Gao, G., Jang, J.N., and Cho, D.W. (2021). Engineering of diseased human skin equivalent using 3D cell printing for representing pathophysiological hallmarks of type 2 diabetes in vitro. Biomaterials *272*, 120776. https://doi.org/10.1016/j.biomaterials.2021.120776.

Kim, H., Kim, Y., Fendereski, M., Hwang, N.S., and Hwang, Y. (2018a). Recent advancements in decellularized matrix-based biomaterials for musculoskeletal tissue regeneration. Adv. Exp. Med. Biol. *1077*, 149–162. https://doi.org/10.1007/978-981-13-0947-2_9.

Kim, J., McBride, S., Tellis, B., Alvarez-Urena, P., Song, Y.H., Dean, D.D., Sylvia, V.L., Elgendy, H., Ong, J., and Hollinger, J.O. (2012a). Rapid-prototyped PLGA/β-TCP/hydroxyapatite nanocomposite scaffolds in a rabbit femoral defect model. Biofabrication *4*, 025003. https://doi.org/10.1088/1758-5082/4/2/025003.

Kim, J.Y., Ahn, G., Kim, C., Lee, J.S., Lee, I.G., An, S.H., Yun, W.S., Kim, S.Y., and Shim, J.H. (2018b). Synergistic effects of beta tri-calcium phosphate and porcine-derived decellularized bone extracellular matrix in 3D-printed polycaprolactone scaffold on bone regeneration. Macromolecular Biosci *18*, 1800025. https://doi.org/10.1002/mabi.201800025.

Kim, K., Dean, D., Wallace, J., Breithaupt, R., Mikos, A., and Fisher, J. (2011). The influence of stereolithographic scaffold architecture and composition on osteogenic signal expression with rat bone marrow stromal cells. Biomaterials *32*, 3750–3763. https://doi.org/10.1016/j.biomaterials.2011.01.016.

Kim, M., Hong, B., Lee, J., Kim, S., Kang, S., Kim, Y., and Tae, G. (2012b). Composite system of PLCL scaffold and heparin-based hydrogel for regeneration of partial-thickness cartilage defects. Biomacromolecules *13*, 2287–2298. https://doi.org/10.1021/bm3005353.

Kim, S., Pan, C.C., and Yang, Y.P. (2020b). Development of a dual hydrogel model system for vascularization. Macromol Biosci *20*, e2000204. https://doi.org/10.1002/mabi.202000204.

Kim, W., and Kim, G. (2020). Collagen/bioceramic-based composite bioink to fabricate a porous 3D hASCs-laden structure for bone

tissue regeneration. Biofabrication *12*, 015007. https://doi.org/10.1088/1758-5090/ab436d.

Kim, W., Lee, H., Lee, J., Atala, A., Yoo, J.J., Lee, S.J., and Kim, G.H. (2020c). Efficient myotube formation in 3D bioprinted tissue construct by biochemical and topographical cues. Biomaterials *230*, 119632. https://doi.org/10.1016/j.biomaterials.2019.119632.

Kim, W., Yun, H., and Kim, G. (2017). An innovative cell-laden alpha-TCP/collagen scaffold fabricated using a two-step printing process for potential application in regenerating hard tissues. Scientific Reports *7*, 3181. https://doi.org/10.1038/s41598-017-03455-9.

Kim, Y.S., Majid, M., Melchiorri, A.J., and Mikos, A.G. (2019). Applications of decellularized extracellular matrix in bone and cartilage tissue engineering. Bioeng Transl Med. *4*, 83–95. https://doi.org/10.1002/btm2.10110.

Klotz, B., Gawlitta, D., Rosenberg, A., Malda, J., and Melchels, F. (2016). Gelatin-methacryloyl hydrogels: towards biofabrication-based tissue repair. Trends Biotechnol. *34*, 394–407. https://doi.org/10.1016/j.tibtech.2016.01.002.

Koch, L., Deiwick, A., Schlie, S., Michael, S., Gruene, M., Coger, V., Zychlinski, D., Schambach, A., Reimers, K., Vogt, P., and Chichkov, B. (2012). Skin tissue generation by laser cell printing. Biotechnol. Bioeng. *109*, 1855–1863. https://doi.org/10.1002/bit.24455.

Koch, L., Kuhn, S., Sorg, H., Gruene, M., Schlie, S., Gaebel, R., Polchow, B., Reimers, K., Stoelting, S., Ma, N., et al. (2010). Laser printing of skin cells and human stem cells. Tissue Eng. Part C-Methods *16*, 847–854. https://doi.org/10.1089/ten.tec.2009.0397.

Kolesky, D., Homan, K., Skylar-Scott, M., and Lewis, J. (2016). Three-dimensional bioprinting of thick vascularized tissues. Proc. Natl. Acad. Sci. United States America *113*, 3179–3184. https://doi.org/10.1073/pnas.1521342113.

Kolesky, D., Truby, R., Gladman, A., Busbee, T., Homan, K., and Lewis, J. (2014). 3D bioprinting of vascularized, heterogeneous cell-laden tissue constructs. Adv. Mater. *26*, 3124–3130. https://doi.org/10.1002/adma.201305506.

Krainer, S., Smit, C., and Hirn, U. (2019). The effect of viscosity and surface tension on inkjet printed picoliter dots. Rsc Adv. *9*, 31708–31719. https://doi.org/10.1039/c9ra04993b.

Kundu, J., Shim, J., Jang, J., Kim, S., and Cho, D. (2015). An additive manufacturing-based PCL-alginate-chondrocyte bioprinted scaffold for cartilage tissue engineering. J. Tissue Eng. Regenerative Med. *9*, 1286–1297. https://doi.org/10.1002/term.1682.

Kwon, D.R., Jung, S., Jang, J., Park, G.Y., Moon, Y.S., and Lee, S.C. (2020). A 3-dimensional bioprinted scaffold with human umbilical cord blood-mesenchymal stem cells improves regeneration of chronic full-thickness rotator cuff tear in a rabbit model. Am. J. Sport Med. *48*, 947–958. https://doi.org/10.1177/0363546520904022.

Lakshminarayan, U., and Marcus, H.L. (1991). Microstructural and mechanical properties of Al2O3/P2O5 and Al2O3/B2O3 composties fabricated by selective laser sintering. In 1991 International Solid Freeform Fabrication Symposium.

Lakshminarayan, U., Ogrydiziak, S., and Marcus, H.L. (1990). Selective Laser Sintering of Ceramic Materials. In 1990 International Solid Freeform Fabrication Symposium.

Lam, C.X., Hutmacher, D.W., Schantz, J.T., Woodruff, M.A., and Teoh, S.H. (2009). Evaluation of polycaprolactone scaffold degradation for 6 months in vitro and in vivo. J Biomed. Mater. Res. A. *90*, 906–919. https://doi.org/10.1002/jbm.a.32052.

Lan, P.X., Lee, J.W., Seol, Y.J., and Cho, D.W. (2009). Development of 3D PPF/DEF scaffolds using micro-stereolithography and surface modification. J. Mater. Sci. Mater. Med. *20*, 271–279. https://doi.org/10.1007/s10856-008-3567-2.

LaNasa, S.M., Hoffecker, I.T., and Bryant, S.J. (2011). Presence of pores and hydrogel composition influence tensile properties of scaffolds fabricated from well-defined sphere templates. J. Biomed. Mater. Res. Part B-Applied Biomater. *96b*, 294–302. https://doi.org/10.1002/jbm.b.31765.

Laternser, S., Keller, H., Leupin, O., Rausch, M., Graf-Hausner, U., and Rimann, M. (2018). A novel microplate 3D bioprinting platform for the engineering of muscle and tendon tissues. Slas Technology *23*, 599–613. https://doi.org/10.1177/2472630318776594.

Lee, H., Ahn, S., Bonassar, L., and Kim, G. (2013). Cell(MC3T3-E1)-Printed poly(epsilon-caprolactone)/alginate hybrid scaffolds for tissue regeneration. Macromolecular Rapid Commun. *34*, 142–149. https://doi.org/10.1002/marc.201200524.

Lee, J., Kang, K., Lee, S., Kim, J., Lee, B., and Cho, D. (2011). Bone regeneration using a microstereolithography-produced customized poly(propylene fumarate)/diethyl fumarate photopolymer 3D scaffold incorporating BMP-2 loaded PLGA microspheres. Biomaterials *32*, 744–752. https://doi.org/10.1016/j.biomaterials.2010.09.035.

Lee, J., Lan, P., Kim, B., Lim, G., and Cho, D. (2008). Fabrication and characteristic analysis of a poly(propylene fumarate) scaffold using micro-stereolithography technology. J. Biomed. Mater. Res. Part B-Applied Biomater. *87B*, 1–9. https://doi.org/10.1002/jbm.b.31057.

Lee, K., and Mooney, D. (2012). Alginate: properties and biomedical applications. Prog. Polym. Sci. *37*, 106–126. https://doi.org/10.1016/j.progpolymsci.2011.06.003.

Lee, K., Wang, S., Fox, B., Ritman, E., Yaszemski, M., and Lu, L. (2007). Poly(propylene fumarate) bone tissue engineering scaffold fabrication using stereolithography: effects of resin formulations and laser parameters. Biomacromolecules *8*, 1077–1084. https://doi.org/10.1021/bm060834v.

Lee, K., Wang, S., Lu, L., Jabbari, E., Currier, B., and Yaszemski, M. (2006). Fabrication and characterization of poly(propylene fumarate) scaffolds with controlled pore structures using 3-dimensional printing and injection molding. Tissue Eng. *12*, 2801–2811. https://doi.org/10.1089/ten.2006.12.2801.

Lee, V., Lanzi, A., Ngo, H., Yoo, S., Vincent, P., and Dai, G. (2014a). Generation of multi-scale vascular network system within 3D hydrogel using 3D bio-printing technology. Cell Mol. Bioeng. *7*, 460–472. https://doi.org/10.1007/s12195-014-0340-0.

Lee, V., Singh, G., Trasatti, J., Bjornsson, C., Xu, X., Tran, T., Yoo, S., Dai, G., and Karande, P. (2014b). Design and abrication of human skin by three-dimensional bioprinting. Tissue Eng. Part C-Methods *20*, 473–484. https://doi.org/10.1089/ten.tec.2013.0335.

Lee, W., Debasitis, J., Lee, V., Lee, J., Fischer, K., Edminster, K., Park, J., and Yoo, S. (2009). Multi-layered culture of human skin fibroblasts and keratinocytes through three-dimensional freeform fabrication. Biomaterials *30*, 1587–1595. https://doi.org/10.1016/j.biomaterials.2008.12.009.

Lee, Y., Polio, S., Lee, W., Dai, G., Menon, L., Carroll, R., and Yoo, S. (2010). Bio-printing of collagen and VEGF-releasing fibrin gel scaffolds for neural stem cell culture. Exp. Neurol. *223*, 645–652. https://doi.org/10.1016/j.expneurol.2010.02.014.

Lewis, P.L., Green, R.M., and Shah, R.N. (2018). 3D-printed gelatin scaffolds of differing pore geometry modulate hepatocyte function and gene expression. Acta Biomater. *69*, 63–70. https://doi.org/10.1016/j.actbio.2017.12.042.

Li, A., Si, Y., Wang, X., Jia, X., Guo, X., and Xu, Y. (2019a). Poly(vinyl alcohol) nanocrystal-assisted hydrogels with high toughness and elastic modulus for three-dimensional printing. Acs Appl. Nano Mater. *2*, 707–715. https://doi.org/10.1021/acsanm.8b01786.

Li, J., de Wijn, J., Van Blitterswijk, C., and de Groot, K. (2006). Porous Ti6Al4V scaffold directly fabricating by rapid prototyping: preparation and in vitro experiment. Biomaterials *27*, 1223–1235. https://doi.org/10.1016/j.biomaterials.2005.08.033.

Li, J., Habibovic, P., Yuan, H., van den Doel, M., Wilson, C., de Wijn, J., van Blitterswijk, C., and de Groot, K. (2007). Biological performance in goats of a porous titanium alloy-biphasic calcium phosphate composite. Biomaterials *28*, 4209–4218. https://doi.org/10.1016/j.biomaterials.2007.05.042.

Li, J., Wu, C., Chu, P., and Gelinsky, M. (2020). 3D printing of hydrogels: rational design strategies and emerging biomedical applications. Mater. Sci. Eng. R-Reports *140*, 100543. UNSP. https://doi.org/10.1016/j.mser.2020.100543.

Li, J.N., Carney, R.P., Liu, R.W., Fan, J.Z., Zhao, S.W., Chen, Y., Lam, K.S., and Pan, T.R. (2018a). Microfluidic print-to-synthesis platform for efficient preparation and screening of combinatorial peptide microarrays. Anal. Chem. *90*, 5833–5840. https://doi.org/10.1021/acs.analchem.8b00371.

Li, J.N., Tan, W., Xiao, W.W., Carney, R.P., Men, Y.F., Li, Y.P., Quon, G., Ajena, Y., Lam, K.S., and Pan, T.R. (2018b). A plug-and-play, drug-on-pillar platform for combination drug screening implemented by microfluidic adaptive printing.

Anal. Chem. *90*, 13969–13977. https://doi.org/10.1021/acs.analchem.8b03456.

Li, M., Benn, F., Derra, T., Kroger, N., Zinser, M., Smeets, R., Molina-Aldareguia, J., Kopp, A., and LLorca, J. (2021). Microstructure, mechanical properties, corrosion resistance and cytocompatibility of WE43 Mg alloy scaffolds fabricated by laser powder bed fusion for biomedical applications. Mater. Sci. Eng. C-Materials Biol. Appl. *119*, 111623. https://doi.org/10.1016/j.msec.2020.111623.

Li, Q., Lei, X., Wang, X., Cai, Z., Lyu, P., and Zhang, G. (2019b). Hydroxyapatite/collagen three-dimensional printed scaffolds and their osteogenic effects on human bone marrow-derived mesenchymal stem cells. Tissue Eng. Part a *25*, 1261–1271. https://doi.org/10.1089/ten.tea.2018.0201.

Li, S., Xiong, Z., Wang, X., Yan, Y., Liu, H., and Zhang, R. (2009). Direct fabrication of a hybrid cell/hydrogel construct by a double-nozzle assembling technology. J. Bioactive Compatible Polym. *24*, 249–265. https://doi.org/10.1177/0883911509104094.

Li, V., Kuang, X., Mulyadi, A., Hamel, C., Deng, Y., and Qi, H. (2019c). 3D printed cellulose nanocrystal composites through digital light processing. Cellulose *26*, 3973–3985. https://doi.org/10.1007/s10570-019-02353-9.

Li, X., Li, D., Lu, B., and Wang, C. (2008). Fabrication of bioceramic scaffolds with pre-designed internal architecture by gel casting and indirect stereolithography techniques. J. Porous Mater. *15*, 667–671. https://doi.org/10.1007/s10934-007-9148-9.

Lim, K.S., Levato, R., Costa, P.F., Castilho, M.D., Alcala-Orozco, C.R., van Dorenmalen, K.M.A., Melchels, F.P.W., Gawlitta, D., Hooper, G.J., Malda, J., and Woodfield, T.B.F. (2018a). Bio-resin for high resolution lithography-based biofabrication of complex cell-laden constructs. Biofabrication *10*, 034101. https://doi.org/10.1088/1758-5090/aac00c.

Lim, K.S., Levato, R., Costa, P.F., Castilho, M.D., Alcala-Orozco, C.R., van Dorenmalen, K.M.A., Melchels, F.P.W., Gawlitta, D., Hooper, G.J., Malda, J., and Woodfield, T.B.F. (2018b). Bio-resin for high resolution lithography-based biofabrication of complex cell-laden constructs. Biofabrication *10*, 034101. https://doi.org/10.1088/1758-5090/aac00c.

Limmahakhun, S., Oloyede, A., Sitthiseripratip, K., Xiao, Y., and Yan, C. (2017). Stiffness and strength tailoring of cobalt chromium graded cellular structures for stress-shielding reduction. Mater. Des. *114*, 633–641. https://doi.org/10.1016/j.matdes.2016.11.090.

Liu, W., Heinrich, M., Zhou, Y., Akpek, A., Hu, N., Liu, X., Guan, X., Zhong, Z., Jin, X., Khademhosseini, A., and Zhang, Y. (2017). Extrusion bioprinting of shear-thinning gelatin methacryloyl bioinks. Adv. Healthc. Mater *6*, 1601451. https://doi.org/10.1002/adhm.201601451.

Liu, X., Rahaman, M.N., Hilmas, G.E., and Bal, B.S. (2013). Mechanical properties of bioactive glass (13-93) scaffolds fabricated by robotic deposition for structural bone repair. Acta Biomater. *9*, 7025–7034. https://doi.org/10.1016/j.actbio.2013.02.026.

Lopez-Heredia, M., Goyenvalle, E., Aguado, E., Pilet, P., Leroux, C., Dorget, M., Weiss, P., and Layrolle, P. (2008). Bone growth in rapid prototyped porous titanium implants. J. Biomed. Mater. Res. Part a *85A*, 664–673. https://doi.org/10.1002/jbm.a.31468.

Lopez-Marcial, G., Zeng, A., Osuna, C., Dennis, J., Garcia, J., and O'Connell, G. (2018). Agarose-based hydrogels as suitable bioprinting materials for tissue engineering. Acs Biomater. Sci. Eng. *4*, 3610–3616. https://doi.org/10.1021/acsbiomaterials.8b00903.

Lu, L., Zhang, Q., Wootton, D., Chiou, R., Li, D., Lu, B., Lelkes, P., and Zhou, J. (2012). Biocompatibility and biodegradation studies of PCL/β-TCP bone tissue scaffold fabricated by structural porogen method. J. Mater. Sci. Mater. Med. *23*, 2217–2226. https://doi.org/10.1007/s10856-012-4695-2.

Lu, Y., Mapili, G., Suhali, G., Chen, S., and Roy, K. (2006). A digital micro-mirror device-based system for the microfabrication of complex, spatially patterned tissue engineering scaffolds. J. Biomed. Mater. Res. Part a *77A*, 396–405. https://doi.org/10.1002/jbm.a.30601.

Lueck, R.A., Galante, J., Rostoker, W., and Ray, R.D. (1969). Development of an open pore metallic implant to permit attachment to bone. Surg. Forum *20*, 456–457.

Luo, Y., Le Fer, G., Dean, D., and Becker, M. (2019a). 3D printing of poly(propylene fumarate) oligomers: evaluation of resin viscosity, printing characteristics and mechanical properties. Biomacromolecules *20*, 1699–1708. https://doi.org/10.1021/acs.biomac.9b00076.

Luo, Y., Le Fer, G., Dean, D., and Becker, M.L. (2019b). 3D printing of poly(propylene fumarate) oligomers: evaluation of resin viscosity, printing characteristics and mechanical properties. Biomacromolecules *20*, 1699–1708. https://doi.org/10.1021/acs.biomac.9b00076.

Luo, Y., Wu, C., Lode, A., and Gelinsky, M. (2013). Hierarchical mesoporous bioactive glass/alginate composite scaffolds fabricated by three-dimensional plotting for bone tissue engineering. Biofabrication *5*, 015005. https://doi.org/10.1088/1758-5082/5/1/015005.

Mamaghani, K., Naghib, S., Zahedi, A., and Mozafari, M. (2018). Synthesis and microstructural characterization of GelMa/PEGDA hybrid hydrogel containing graphene oxide for biomedical purposes. Mater. Today-Proceedings *5*, 15635–15644. https://doi.org/10.1016/j.matpr.2018.04.173.

Mariani, L., Johnson, W., Considine, J., and Turner, K. (2019). Printing and mechanical characterization of cellulose nanofibril materials. Cellulose *26*, 2639–2651. https://doi.org/10.1007/s10570-019-02247-w.

Markstedt, K., Mantas, A., Tournier, I., Martínez Ávila, H., Hägg, D., and Gatenholm, P. (2015). 3D bioprinting human chondrocytes with nanocellulose-alginate bioink for cartilage tissue engineering applications. Biomacromolecules *16*, 1489–1496. https://doi.org/10.1021/acs.biomac.5b00188.

Maruyama, M., Nabeshima, A., Pan, C., Behn, A., Thio, T., Lin, T., Pajarinen, J., Kawai, T., Takagi, M., Goodman, S., and Yang, Y. (2018). The effects of a functionally-graded scaffold and bone marrow-derived mononuclear cells on steroid-induced femoral head osteonecrosis. Biomaterials *187*, 39–46. https://doi.org/10.1016/j.biomaterials.2018.09.030.

Masood, S., Singh, J., and Morsi, Y. (2005). The design and manufacturing of porous scaffolds for tissue engineering using rapid prototyping. Int. J. Adv. Manufacturing Technology *27*, 415–420. https://doi.org/10.1007/s00170-004-2187-3.

Melchels, F., Domingos, M., Klein, T., Malda, J., Bartolo, P., and Hutmacher, D. (2012). Additive manufacturing of tissues and organs. Prog. Polym. Sci. *37*, 1079–1104. https://doi.org/10.1016/j.progpolymsci.2011.11.007.

Melchiorri, A.J., Hibino, N., Best, C.A., Yi, T., Lee, Y.U., Kraynak, C.A., Kimerer, L.K., Krieger, A., Kim, P., Breuer, C.K., and Fisher, J.P. (2016). 3D-Printed biodegradable polymeric vascular grafts. Adv. Healthc. Mater. *5*, 319–325. https://doi.org/10.1002/adhm.201500725.

Melican, M., Zimmerman, M., Dhillon, M., Ponnambalam, A., Curodeau, A., and Parsons, J. (2001). Three-dimensional printing and porous metallic surfaces: a new orthopedic application. J. Biomed. Mater. Res. *55*, 194–202. https://doi.org/10.1002/1097-4636(200105)55:2<194::AID-JBM1006>3.0.CO;2-K.

Meng, Y., Cao, J., Chen, Y., Yu, Y., and Ye, L. (2020). 3D printing of a poly(vinyl alcohol)-based nano-composite hydrogel as an artificial cartilage replacement and the improvement mechanism of printing accuracy. J. Mater. Chem. B *8*, 677–690. https://doi.org/10.1039/c9tb02278c.

Mercado-Pagán, Á., Stahl, A.M., Shanjani, Y., and Yang, Y. (2015). Vascularization in bone tissue engineering constructs. Ann. Biomed. Eng. *43*, 718–729. https://doi.org/10.1007/s10439-015-1253-3.

Michael, S., Sorg, H., Peck, C., Koch, L., Deiwick, A., Chichkov, B., Vogt, P., and Reimers, K. (2013). Tissue engineered skin substitutes created by laser-assisted bioprinting form skin-like structures in the dorsal skin fold chamber in mice. Plos One *8*, e57741. https://doi.org/10.1371/journal.pone.0057741.

Min, D., Lee, W., Bae, I., Lee, T., Croce, P., and Yoo, S. (2018). Bioprinting of biomimetic skin containing melanocytes. Exp. Dermatol. *27*, 453–459. https://doi.org/10.1111/exd.13376.

Mintz, B., and Cooper, J. (2014). Hybrid hyaluronic acid hydrogel/poly(epsilon-caprolactone) scaffold provides mechanically favorable platform for cartilage tissue engineering studies. J. Biomed. Mater. Res. Part a *102*, 2918–2926. https://doi.org/10.1002/jbm.a.34957.

Mishra, R., Roux, B.M., Posukonis, M., Bodamer, E., Brey, E.M., Fisher, J.P., and Dean, D. (2016). Effect of prevascularization on in vivo vascularization of poly(propylene fumarate)/fibrin scaffolds. Biomaterials *77*, 255–266. https://doi.org/10.1016/j.biomaterials.2015.10.026.

Mondschein, R.J., Kanitkar, A., Williams, C.B., Verbridge, S.S., and Long, T.E. (2017). Polymer

structure-property requirements for stereolithographic 3D printing of soft tissue engineering scaffolds. Biomaterials *140*, 170–188. https://doi.org/10.1016/j.biomaterials.2017.06.005.

Moon, S., Hasan, S., Song, Y., Xu, F., Keles, H., Manzur, F., Mikkilineni, S., Hong, J., Nagatomi, J., Haeggstrom, E., et al. (2010). Layer by layer three-dimensional tissue epitaxy by cell-laden hydrogel droplets. Tissue Eng. Part C-Methods *16*, 157–166. https://doi.org/10.1089/ten.tec.2009.0179.

Morris, V., Nimbalkar, S., Younesi, M., McClellan, P., and Akkus, O. (2017). Mechanical properties, cytocompatibility and manufacturability of chitosan:PEGDA hybrid-gel scaffolds by stereolithography. Ann. Biomed. Eng. *45*, 286–296. https://doi.org/10.1007/s10439-016-1643-1.

Müller, M., Öztürk, E., Arlov, Ø., Gatenholm, P., and Zenobi-Wong, M. (2017). Alginate sulfate-nanocellulose bioinks for cartilage bioprinting applications. Ann. Biomed. Eng. *45*, 210–223. https://doi.org/10.1007/s10439-016-1704-5.

Muralidharan, A., Uzcategui, A.C., McLeod, R.R., and Bryant, S.J. (2019). Stereolithographic 3D printing for deterministic control over integration in dual-material composites. Adv. Mater. Technol. *4*. https://doi.org/10.1002/admt.201900592.

Murphy, C., Kolan, K., Li, W.B., Semon, J., Day, D., and Leu, M. (2017). 3D bioprinting of stem cells and polymer/bioactive glass composite scaffolds for bone tissue engineering. Int. J. Bioprinting *3*, 54–64. https://doi.org/10.18063/ljb.2017.01.005.

Murphy, S.V., Skardal, A., and Atala, A. (2013). Evaluation of hydrogels for bio-printing applications. J. Biomed. Mater. Res. A. *101*, 272–284. https://doi.org/10.1002/jbm.a.34326.

Nadernezhad, A., Caliskan, O., Topuz, F., Afghah, F., Erman, B., and Koc, B. (2019). Nanocomposite bioinks based on agarose and 2D nanosilicates with tunable flow properties and bioactivity for 3D bioprinting. Acs Appl. Bio Mater. *2*, 796–806. https://doi.org/10.1021/acsabm.8b00665.

Nettleton, K., Luong, D., Kleinfehn, A., Savariau, L., Premanandan, C., and Becker, M. (2019). Molecular mass-dependent resorption and bone regeneration of 3D printed PPF scaffolds in a critical-sized rat cranial defect model. Adv. Healthc. Mater *8*, 1900646. https://doi.org/10.1002/adhm.201900646.

Neufurth, M., Wang, X., Schröder, H.C., Feng, Q., Diehl-Seifert, B., Ziebart, T., Steffen, R., Wang, S., and Müller, W.E.G. (2014). Engineering a morphogenetically active hydrogel for bioprinting of bioartificial tissue derived from human osteoblast-like SaOS-2 cells. Biomaterials *35*, 8810–8819. https://doi.org/10.1016/j.biomaterials.2014.07.002.

Nguyen, Q.T., Hwang, Y., Chen, A.C., Varghese, S., and Sah, R.L. (2012). Cartilage-like mechanical properties of poly (ethylene glycol)-diacrylate hydrogels. Biomaterials *33*, 6682–6690. https://doi.org/10.1016/j.biomaterials.2012.06.005.

Nichol, J.W., Koshy, S.T., Bae, H., Hwang, C.M., Yamanlar, S., and Khademhosseini, A. (2010). Cell-laden microengineered gelatin methacrylate hydrogels. Biomaterials *31*, 5536–5544. https://doi.org/10.1016/j.biomaterials.2010.03.064.

Noor, N., Shapira, A., Edri, R., Gal, I., Wertheim, L., and Dvir, T. (2019). 3D printing of personalized thick and perfusable cardiac patches and hearts. Adv. Sci. (Weinh) *6*, 1900344. https://doi.org/10.1002/advs.201900344.

Nordberg, R.C., Bodle, J.C., and Loboa, E.G. (2018). Mechanical stimulation of adipose-derived stem cells for functional tissue engineering of the musculoskeletal system via cyclic hydrostatic pressure, simulated microgravity, and cyclic tensile strain. Methods Mol. Biol. *1773*, 215–230. https://doi.org/10.1007/978-1-4939-7799-4_18.

Nyberg, E., Rindone, A., Dorafshar, A., and Grayson, W.L. (2017). Comparison of 3D-printed poly-epsilon-caprolactone scaffolds functionalized with tricalcium phosphate, hydroxyapatite, bio-oss, or decellularized bone matrix. Tissue Eng. Part A *23*, 503. https://doi.org/10.1089/ten.tea.2016.0418.

Olubamiji, A., Izadifar, Z., Si, J., Cooper, D., Eames, B., and Chen, D. (2016). Modulating mechanical behaviour of 3D-printed cartilage-mimetic PCL scaffolds: influence of molecular weight and pore geometry. Biofabrication *8*, 025020. https://doi.org/10.1088/1758-5090/8/2/025020.

Ostrovidov, S., Salehi, S., Costantini, M., Suthiwanich, K., Ebrahimi, M., Sadeghian, R.B., Fujie, T., Shi, X., Cannata, S., Gargioli, C., et al. (2019). 3D bioprinting in skeletal muscle tissue engineering. Small *15*, e1805530. https://doi.org/10.1002/smll.201805530.

Ovsianikov, A., Deiwick, A., Van Vlierberghe, S., Dubruel, P., Moller, L., Drager, G., and Chichkov, B. (2011). Laser fabrication of three-dimensional CAD scaffolds from photosensitive gelatin for applications in tissue engineering. Biomacromolecules *12*, 851–858. https://doi.org/10.1021/bm1015305.

Ovsianikov, A., Gruene, M., Pflaum, M., Koch, L., Maiorana, F., Wilhelmi, M., Haverich, A., and Chichkov, B. (2010). Laser printing of cells into 3D scaffolds. Biofabrication *2*, 014104. https://doi.org/10.1088/1758-5082/2/1/014104.

Park, J., Shim, J., Choi, S., Jang, J., Kim, M., Lee, S., and Cho, D. (2015). 3D printing technology to control BMP-2 and VEGF delivery spatially and temporally to promote large-volume bone regeneration. J. Mater. Chem. B *3*, 5415–5425. https://doi.org/10.1039/c5tb00637f.

Park, S.A., Lee, S.H., and Kim, W.D. (2011). Fabrication of porous polycaprolactone/hydroxyapatite (PCL/HA) blend scaffolds using a 3D plotting system for bone tissue engineering. Bioproc. Biosyst Eng *34*, 505–513. https://doi.org/10.1007/s00449-010-0499-2.

Park, S.H., Choi, Y.J., Moon, S.W., Lee, B.H., Shim, J.H., Cho, D.W., and Wang, J.H. (2018). Three-dimensional bio-printed scaffold sleeves with mesenchymal stem cells for enhancement of tendon-to-bone healing in anterior cruciate ligament reconstruction using soft-tissue tendon graft. Arthroscopy-the J. Arthroscopic Relat. Surg. *34*, 166–179. https://doi.org/10.1016/j.arthro.2017.04.016.

Parry, J., Olthof, M., Shogren, K., Dadsetan, M., Van Wijnen, A., Yaszemski, M., and Kakar, S. (2017). Three-dimension-printed porous poly(propylene fumarate) scaffolds with delayed rhBMP-2 release for anterior cruciate ligament graft fixation. Tissue Eng. Part a *23*, 359–365. https://doi.org/10.1089/ten.tea.2016.0343.

Pati, F., Jang, J., Ha, D., Kim, S., Rhie, J., Shim, J., Kim, D., and Cho, D. (2014a). Printing three-dimensional tissue analogues with decellularized extracellular matrix bioink. Nat. Commun *5*, 3935. https://doi.org/10.1038/ncomms4935.

Pati, F., Jang, J., Ha, D.H., Kim, S.W., Rhie, J.W., Shim, J.H., Kim, D.H., and Cho, D.W. (2014b). Printing three-dimensional tissue analogues with decellularized extracellular matrix bioink. Nat. Commun *5*, 3935. https://doi.org/10.1038/ncomms4935.

Pecqueux, F., Tancret, F., Payraudeau, N., and Bouler, J.M. (2010). Influence of microporosity and macroporosity on the mechanical properties of biphasic calcium phosphate bioceramics: modelling and experiment. J. Eur. Ceram. Soc. *30*, 819–829. https://doi.org/10.1016/j.jeurceramsoc.2009.09.017.

Peele, B.N., Wallin, T.J., Zhao, H.C., and Shepherd, R.F. (2015). 3D printing antagonistic systems of artificial muscle using projection stereolithography. Bioinspir Biomim *10*, 055003. https://doi.org/10.1088/1748-3190/10/5/055003.

Percoco, G., Uva, A.E., Fiorentino, M., Gattullo, M., Manghisi, V.M., and Boccaccio, A. (2020). Mechanobiological approach to design and optimize bone tissue scaffolds 3D printed with fused deposition modeling: a feasibility study. Materials *13*, 648. https://doi.org/10.3390/ma13030648.

Phillippi, J.A., Miller, E., Weiss, L., Huard, J., Waggoner, A., and Campbell, P. (2008). Microenvironments engineered by inkjet bioprinting spatially direct adult stem cells toward muscle- and bone-like subpopulations. Stem Cells *26*, 127–134. https://doi.org/10.1634/stemcells.2007-0520.

Place, E., George, J., Williams, C., and Stevens, M. (2009). Synthetic polymer scaffolds for tissue engineering. Chem. Soc. Rev. *38*, 1139–1151. https://doi.org/10.1039/b811392k.

Place, E.S., Rojo, L., Gentleman, E., Sardinha, J.P., and Stevens, M.M. (2011). Strontium- and zinc-alginate hydrogels for bone tissue engineering. Tissue Eng. Part A. *17*, 2713–2722. https://doi.org/10.1089/ten.TEA.2011.0059.

Puertolas, J.A., Vadillo, J.L., Sanchez-Salcedo, S., Nieto, A., Gomez-Barrena, E., and Vallet-Regi, M. (2011). Compression behaviour of biphasic calcium phosphate and biphasic calcium phosphate-agarose scaffolds for bone regeneration. Acta Biomater. *7*, 841–847. https://doi.org/10.1016/j.actbio.2010.07.032.

Qayyum, A., Jain, E., Kolar, G., Kim, Y., Sell, S., and Zustiak, S. (2017). Design of electrohydrodynamic sprayed polyethylene glycol hydrogel microspheres for cell encapsulation. Biofabrication *9*, 025019. https://doi.org/10.1088/1758-5090/aa703c.

Qi, X.P., and Ye, J.D. (2009). Mechanical and rheological properties and injectability of calcium

phosphate cement containing poly (lactic-co-glycolic acid) microspheres. Mater. Sci. Eng. C-Materials Biol. Appl. *29*, 1901–1906. https://doi.org/10.1016/j.msec.2009.02.021.

Qian, G., Zhang, L., Wang, G., Zhao, Z., Peng, S., and Shuai, C. (2021). 3D printed Zn-doped mesoporous silica-incorporated poly-L-lactic acid scaffolds for bone repair. Int. J. Bioprinting *7*, 92–103. https://doi.org/10.18063/ijb.v7i2.346.

Rajaram, A., Schreyer, D., and Chen, D. (2014). Bioplotting alginate/hyaluronic acid hydrogel scaffolds with structural integrity and preserved schwann cell viability. 3d Printing and Additive Manufacturing *1*, 194–203. https://doi.org/10.1089/3dp.2014.0006.

Rak Kwon, D., Jung, S., Jang, J., Park, G.-Y., Suk Moon, Y., and Lee, S.C. (2020). A 3-dimensional bioprinted scaffold with human umbilical cord blood–mesenchymal stem cells improves regeneration of chronic full-thickness rotator cuff tear in a rabbit model. Am. J. Sports Med. *48*, 947–958. https://doi.org/10.1177/0363546520904022.

Rasoulianboroujeni, M., Fahimipour, F., Shah, P., Khoshroo, K., Tahriri, M., Eslami, H., Yadegari, A., Dashtimoghadam, E., and Tayebi, L. (2019). Development of 3D-printed PLGA/TiO2 nano-composite scaffolds for bone tissue engineering applications. Mater. Sci. Eng. C-Materials Biol. Appl. *96*, 105–113. https://doi.org/10.1016/j.msec.2018.10.077.

Reakasame, S., and Boccaccini, A.R. (2018). Oxidized alginate-based hydrogels for tissue engineering applications: a review. Biomacromolecules *19*, 3–21. https://doi.org/10.1021/acs.biomac.7b01331.

Ren, X., Wang, F., Chen, C., Gong, X., Yin, L., and Yang, L. (2016). Engineering zonal cartilage through bioprinting collagen type II hydrogel constructs with biomimetic chondrocyte density gradient. Bmc Musculoskelet. Disorders *17*, 301. https://doi.org/10.1186/s12891-016-1130-8.

Rhee, S., Puetzer, J., Mason, B., Reinhart-King, C., and Bonassar, L. (2016). 3D bioprinting of spatially heterogeneous collagen constructs for cartilage tissue engineering. Acs Biomater. Sci. Eng. *2*, 1800–1805. https://doi.org/10.1021/acsbiomaterials.6b00288.

Rho, J.Y., Ashman, R.B., and Turner, C.H. (1993). Young's modulus of trabecular and cortical bone material: ultrasonic and microtensile measurements. J. Biomech. *26*, 111–119. https://doi.org/10.1016/0021-9290(93)90042-d.

Rho, J.Y., Roy, M.E., Tsui, T.Y., and Pharr, G.M. (1999). Elastic properties of microstructural components of human bone tissue as measured by nanoindentation. J. Biomed. Mater. Res. *45*, 48–54. https://doi.org/10.1002/(sici)1097-4636(199904)45:1<48::aid-jbm7>3.0.co;2-5.

Rho, J.Y., Tsui, T.Y., and Pharr, G.M. (1997). Elastic properties of human cortical and trabecular lamellar bone measured by nanoindentation. Biomaterials *18*, 1325–1330. https://doi.org/10.1016/s0142-9612(97)00073-2.

Rimann, M., Bono, E., Annaheim, H., Bleisch, M., and Graf-Hausner, U. (2016). Standardized 3D bioprinting of soft tissue models with human primary cells. Jala *21*, 496–509. https://doi.org/10.1177/2211068214567146.

Rimington, R.P., Capel, A.J., Christie, S.D.R., and Lewis, M.P. (2017). Biocompatible 3D printed polymers via fused deposition modelling direct C2C12 cellular phenotype in vitro. Lab A Chip *17*, 2982–2993. https://doi.org/10.1039/c7lc00577f.

Ringeisen, B.R., Kim, H., Barron, J.A., Krizman, D.B., Chrisey, D.B., Jackman, S., Auyeung, R.Y., and Spargo, B.J. (2004). Laser printing of pluripotent embryonal carcinoma cells. Tissue Eng. *10*, 483–491. https://doi.org/10.1089/107632704323061843.

Roberts, J.J., Earnshaw, A., Ferguson, V.L., and Bryant, S.J. (2011). Comparative study of the viscoelastic mechanical behavior of agarose and poly(ethylene glycol) hydrogels. J. Biomed. Mater. Res. B Appl. Biomater. *99*, 158–169. https://doi.org/10.1002/jbm.b.31883.

Romanazzo, S., Molley, T.G., Nemec, S., Lin, K., Sheikh, R., Gooding, J.J., Wan, B.Y., Li, Q., Kilian, K.A., and Roohani, I. (2021). Synthetic bone-like structures through omnidirectional ceramic bioprinting in cell suspensions. Adv. Funct. Mater *31*, 2008216. https://doi.org/10.1002/adfm.202008216.

Rosenzweig, D.H., Carelli, E., Steffen, T., Jarzem, P., and Haglund, L. (2015). 3D-Printed ABS and PLA scaffolds for cartilage and nucleus pulposus tissue regeneration. Int. J. Mol. Sci. *16*, 15118–15135. https://doi.org/10.3390/ijms160715118.

Ryan, G., Pandit, A., and Apatsidis, D. (2006). Fabrication methods of porous metals for use in orthopaedic applications. Biomaterials *27*, 2651–2670. https://doi.org/10.1016/j.biomaterials.2005.12.002.

Sabir, M., Xu, X., and Li, L. (2009). A review on biodegradable polymeric materials for bone tissue engineering applications. J. Mater. Sci. *44*, 5713–5724. https://doi.org/10.1007/s10853-009-3770-7.

Sadeghianmaryan, A., Naghieh, S., Sardroud, H., Yazdanpanah, Z., Soltani, Y., Sernaglia, J., and Chen, X. (2020). Extrusion-based printing of chitosan scaffolds and their in vitro characterization for cartilage tissue engineering. Int. J. Biol. Macromolecules *164*, 3179–3192. https://doi.org/10.1016/j.ijbiomac.2020.08.180.

Saha, S., Wang, D., Nguyen, V., Chang, Y., Oakdale, J., and Chen, S. (2019). Scalable submicrometer additive manufacturing. Science *366*, 105. https://doi.org/10.1126/science.aax8760.

Sakthiabirami, K., Kang, J.H., Jang, J.G., Soundharrajan, V., Lim, H.P., Yun, K.D., Park, C., Lee, B.N., Yang, Y.P., and Park, S.W. (2021a). Hybrid porous zirconia scaffolds fabricated using additive manufacturing for bone tissue engineering applications. Mater. Sci. Eng. C-Materials Biol. Appl *123*, 111950. https://doi.org/10.1016/j.msec.2021.111950.

Sakthiabirami, K., Soundharrajan, V., Kang, J.H., Yang, Y.P., and Park, S.W. (2021b). Three-dimensional zirconia-based scaffolds for load-bearing bone-regeneration applications: prospects and challenges. Materials *14*, 3207. https://doi.org/10.3390/ma14123207.

Salehi, M., Maleksaeedi, S., Bin Sapari, M., Nai, M., Meenashisundaram, G., and Gupta, M. (2019a). Additive manufacturing of magnesium-zinc-zirconium (ZK) alloys via capillary-mediated binderless three-dimensional printing. Mater. Des *169*, 107683. https://doi.org/10.1016/j.matdes.2019.107683.

Salehi, M., Maleksaeedi, S., Nai, M., and Gupta, M. (2019b). Towards additive manufacturing of magnesium alloys through integration of binderless 3D printing and rapid microwave sintering. Additive Manufacturing *29*, 100790. https://doi.org/10.1016/j.addma.2019.100790.

Salerno, A., Fernández-Gutiérrez, M., Barrio, J.S.R.d., and Domingo, C. (2015). Bio-safe fabrication of PLA scaffolds for bone tissue engineering by combining phase separation, porogen leaching and scCO2 drying. J. Supercrit. Fluids *97*, 238–246.

Santos, M., Tuzlakoglu, K., Fuchs, S., Gomes, M., Peters, K., Unger, R., Piskin, E., Reis, R., and Kirkpatrick, C. (2008). Endothelial cell colonization and angiogenic potential of combined nano- and micro-fibrous scaffolds for bone tissue engineering. Biomaterials *29*, 4306–4313. https://doi.org/10.1016/j.biomaterials.2008.07.033.

Schiele, N., Chrisey, D., and Corr, D. (2011). Gelatin-based laser direct-write technique for the precise spatial patterning of cells. Tissue Eng. Part C-Methods *17*, 289–298. https://doi.org/10.1089/ten.tec.2010.0442.

Schiele, N.R., Koppes, R.A., Corr, D.T., Ellison, K.S., Thompson, D.M., Ligon, L.A., Lippert, T.K.M., and Chrisey, D.B. (2009). Laser direct writing of combinatorial libraries of idealized cellular constructs: biomedical applications. Appl. Surf. Sci. *255*, 5444–5447. https://doi.org/10.1016/j.apsusc.2008.10.054.

Schuurman, W., Khristov, V., Pot, M., van Weeren, P., Dhert, W., and Malda, J. (2011). Bioprinting of hybrid tissue constructs with tailorable mechanical properties. Biofabrication *3*, 021001. https://doi.org/10.1088/1758-5082/3/2/021001.

Schuurman, W., Levett, P., Pot, M., van Weeren, P., Dhert, W., Hutmacher, D., Melchels, F., Klein, T., and Malda, J. (2013a). Gelatin-Methacrylamide hydrogels as potential biomaterials for fabrication of tissue-engineered cartilage constructs. Macromolecular Biosci. *13*, 551–561. https://doi.org/10.1002/mabi.201200471.

Schuurman, W., Levett, P.A., Pot, M.W., van Weeren, P.R., Dhert, W.J.A., Hutmacher, D.W., Melchels, F.P.W., Klein, T.J., and Malda, J. (2013b). Gelatin-Methacrylamide hydrogels as potential biomaterials for fabrication of tissue-engineered cartilage constructs. Macromolecular Biosci. *13*, 551–561. https://doi.org/10.1002/mabi.201200471.

Sears, N., Dhavalikar, P., Whitely, M., and Cosgriff-Hernandez, E. (2017). Fabrication of biomimetic bone grafts with multi-material 3D printing. Biofabrication *9*, 025020. https://doi.org/10.1088/1758-5090/aa7077.

Seidlits, S.K., Khaing, Z.Z., Petersen, R.R., Nickels, J.D., Vanscoy, J.E., Shear, J.B., and Schmidt, C.E. (2010). The effects of hyaluronic acid hydrogels with tunable mechanical properties on neural progenitor cell differentiation. Biomaterials *31*,

3930–3940. https://doi.org/10.1016/j.biomaterials.2010.01.125.

Seol, Y., Park, J., Jung, J., Jang, J., Girdhari, R., Kim, S., and Cho, D. (2014). Improvement of bone regeneration capability of ceramic scaffolds by accelerated release of their calcium ions. Tissue Eng. Part a *20*, 2840–2849. https://doi.org/10.1089/ten.tea.2012.0726.

Serafin, A., Murphy, C., Rubio, M., and Collins, M. (2021). Printable alginate/gelatin hydrogel reinforced with carbon nanofibers as electrically conductive scaffolds for tissue engineering. Mater. Sci. Eng. C-Materials Biol. Appl *122*, 111927. https://doi.org/10.1016/j.msec.2021.111927.

Shanjani, Y., Kang, Y., Zarnescu, L., Ellerbee Bowden, A.K., Koh, J.T., Ker, D.F.E., and Yang, Y. (2017). Endothelial pattern formation in hybrid constructs of additive manufactured porous rigid scaffolds and cell-laden hydrogels for orthopedic applications. J. Mech. Behav. Biomed. Mater. *65*, 356–372. https://doi.org/10.1016/j.jmbbm.2016.08.037.

Shanjani, Y., Pan, C., Elomaa, L., and Yang, Y. (2015). A novel bioprinting method and system for forming hybrid tissue engineering constructs. Biofabrication *7*, 045008. https://doi.org/10.1088/1758-5090/7/4/045008.

Shanjani, Y., Siebert, S., Ker, D., Mercado-Pagan, A., and Yang, Y. (2020). Acoustic patterning of growth factor for three-dimensional tissue engineering. Tissue Eng. Part A. https://doi.org/10.1089/ten.tea.2019.0271.

Sharma, R., Kirsch, R., Valente, K., Perez, M., and Willerth, S. (2021). Physical and mechanical characterization of fibrin-based bioprinted constructs containing drug-releasing microspheres for neural tissue engineering applications. Processes *9*, 1205. https://doi.org/10.3390/pr9071205.

Shim, J., Kim, J., Park, M., Park, J., and Cho, D. (2011). Development of a hybrid scaffold with synthetic biomaterials and hydrogel using solid freeform fabrication technology. Biofabrication *3*, 034102. https://doi.org/10.1088/1758-5082/3/3/034102.

Shim, J., Lee, J., Kim, J., and Cho, D. (2012). Bioprinting of a mechanically enhanced three-dimensional dual cell-laden construct for osteochondral tissue engineering using a multi-head tissue/organ building system. J. Micromechanics Microengineering *22*, 085014. https://doi.org/10.1088/0960-1317/22/8/085014.

Shin, S., Bae, H., Cha, J., Mun, J., Chen, Y., Tekin, H., Shin, H., Farshchi, S., Dokmeci, M., Tang, S., and Khademhosseini, A. (2012). Carbon nanotube reinforced hybrid microgels as scaffold materials for cell encapsulation. Acs Nano *6*, 362–372. https://doi.org/10.1021/nn203711s.

Shor, L., Güçeri, S., Chang, R., Gordon, J., Kang, Q., Hartsock, L., An, Y., and Sun, W. (2009). Precision extruding deposition (PED) fabrication of polycaprolactone (PCL) scaffolds for bone tissue engineering. Biofabrication *1*, 015003. https://doi.org/10.1088/1758-5082/1/1/015003.

Skardal, A., Mack, D., Kapetanovic, E., Atala, A., Jackson, J., Yoo, J., and Soker, S. (2012). Bioprinted amniotic fluid-derived stem cells accelerate healing of large skin wounds. Stem Cells Translational Med. *1*, 792–802. https://doi.org/10.5966/sctm.2012-0088.

Skylar-Scott, M., Liu, M., Wu, Y., Dixit, A., and Yanik, M. (2016). Guided homing of cells in multi-photon microfabricated bioscaffolds. Adv. Healthc. Mater. *5*, 1233–1243. https://doi.org/10.1002/adhm.201600082.

Skylar-Scott, M.A., Mueller, J., Visser, C.W., and Lewis, J.A. (2019a). Voxelated soft matter via multimaterial multinozzle 3D printing. Nature *575*, 330–335. https://doi.org/10.1038/s41586-019-1736-8.

Skylar-Scott, M.A., Uzel, S.G.M., Nam, L.L., Ahrens, J.H., Truby, R.L., Damaraju, S., and Lewis, J.A. (2019b). Biomanufacturing of organ-specific tissues with high cellular density and embedded vascular channels. Sci. Adv *5*, eaaw2459. https://doi.org/10.1126/sciadv.aaw2459.

Smith, C.M., Stone, A.L., Parkhill, R.L., Stewart, R.L., Simpkins, M.W., Kachurin, A.M., Warren, W.L., and Williams, S.K. (2004). Three-dimensional bioassembly tool for generating viable tissue-engineered constructs. Tissue Eng. *10*, 1566–1576. https://doi.org/10.1089/ten.2004.10.1566.

Sun, H., Hu, C., Zhou, C., Wu, L., Sun, J., Zhou, X., Xing, F., Long, C., Kong, Q., Liang, J., et al. (2020). 3D printing of calcium phosphate scaffolds with controlled release o antibacterial functions for jaw bone repair. Mater. Des *189*, 108540. https://doi.org/10.1016/j.matdes.2020.108540.

Suo, H., Zhang, J., Xu, M., and Wang, L. (2021). Low-temperature 3D printing of collagen and chitosan composite for tissue engineering. Mater. Sci. Eng. C-Materials Biol. Appl *123*, 111963. https://doi.org/10.1016/j.msec.2021.111963.

Suwanpreecha, C., Alabort, E., Tang, Y., Panwisawas, C., Reed, R., and Manonukul, A. (2021). A novel low-modulus titanium alloy for biomedical applications: a comparison between selective laser melting and metal injection moulding. Mater. Sci. Eng. a-Structural Mater. Properties Microstructure Process *812*, 141081. https://doi.org/10.1016/j.msea.2021.141081.

Swetha, M., Sahithi, K., Moorthi, A., Saranya, N., Saravanan, S., Ramasamy, K., Srinivasan, N., and Selvamurugan, N. (2012). Synthesis, characterization, and antimicrobial activity of nano-hydroxyapatite-zinc for bone tissue engineering applications. J. Nanosci Nanotechnol *12*, 167–172. https://doi.org/10.1166/jnn.2012.5142.

Tabriz, A.G., Hermida, M.A., Leslie, N.R., and Shu, W. (2015). Three-dimensional bioprinting of complex cell laden alginate hydrogel structures. Biofabrication *7*, 045012. https://doi.org/10.1088/1758-5090/7/4/045012.

Tan, G., Zhou, L., Ning, C., Tan, Y., Ni, G., Liao, J., Yu, P., and Chen, X. (2013). Biomimetically-mineralized composite coatings on titanium functionalized with gelatin methacrylate hydrogels. Appl. Surf. Sci. *279*, 293–299. https://doi.org/10.1016/j.apsusc.2013.04.088.

Tan, K.H., Chua, C.K., Leong, K.F., Cheah, C.M., Gui, W.S., Tan, W.S., and Wiria, F.E. (2005). Selective laser sintering of biocompatible polymers for applications in tissue engineering. Biomed. Mater. Eng. *15*, 113–124.

Tarafder, S., Balla, V., Davies, N., Bandyopadhyay, A., and Bose, S. (2013). Microwave-sintered 3D printed tricalcium phosphate scaffolds for bone tissue engineering. J. Tissue Eng. Regenerative Med. *7*, 631–641. https://doi.org/10.1002/term.555.

Tavsanli, B., and Okay, O. (2017). Mechanically strong hyaluronic acid hydrogels with an interpenetrating network structure. Eur. Polym. J. *94*, 185–195. https://doi.org/10.1016/j.eurpolymj.2017.07.009.

Tekinalp, H., Meng, X., Lu, Y., Kunc, V., Love, L., Peter, W., and Ozcan, S. (2019). High modulus biocomposites via additive manufacturing: cellulose nanofibril networks as "microsponges". Composites Part B-Engineering *173*, 106817. https://doi.org/10.1016/j.compositesb.2019.05.028.

Temenoff, J.S., Athanasiou, K.A., LeBaron, R.G., and Mikos, A.G. (2002). Effect of poly(ethylene glycol) molecular weight on tensile and swelling properties of oligo(poly(ethylene glycol) fumarate) hydrogels for cartilage tissue engineering. J. Biomed. Mater. Res. *59*, 429–437. https://doi.org/10.1002/jbm.1259.

Temple, J.P., Hutton, D.L., Hung, B.P., Huri, P.Y., Cook, C.A., Kondragunta, R., Jia, X., and Grayson, W.L. (2014). Engineering anatomically shaped vascularized bone grafts with hASCs and 3D-printed PCL scaffolds. J. Biomed. Mater. Res. A. *102*, 4317–4325. https://doi.org/10.1002/jbm.a.35107.

Tirella, A., Liberto, T., and Ahluwalia, A. (2012). Riboflavin and collagen: new crosslinking methods to tailor the stiffness of hydrogels. Mater. Lett. *74*, 58–61. https://doi.org/10.1016/j.matlet.2012.01.036.

Todros, S., Spadoni, S., Maghin, E., Piccoli, M., and Pavan, P.G. (2021). A novel bioreactor for the mechanical stimulation of clinically relevant scaffolds for muscle tissue engineering purposes. Processes *9*, 474. https://doi.org/10.3390/pr9030474.

Toprakhisar, B., Nadernezhad, A., Bakirci, E., Khani, N., Skvortsov, G., and Koc, B. (2018). Development of bioink from decellularized tendon extracellular matrix for 3D bioprinting. Macromolecular Biosci *18*, 1800024. https://doi.org/10.1002/mabi.201800024.

Touré, A.B.R., Mele, E., and Christie, J.K. (2020). Multi-layer scaffolds of poly(caprolactone), poly(glycerol sebacate) and bioactive glasses manufactured by combined 3D printing and electrospinning. Nanomaterials *10*, 626. https://doi.org/10.3390/nano10040626.

Trachtenberg, J., Placone, J., Smith, B., Piard, C., Santoro, M., Scott, D., Fisher, J., and Mikos, A. (2016). Extrusion-based 3D printing of poly(propylene fumarate) in a full-factorial design. Acs Biomater. Sci. Eng. *2*, 1771–1780. https://doi.org/10.1021/acsbiomaterials.6b00026.

Trachtenberg, J.E., Placone, J.K., Smith, B.T., Fisher, J.P., and Mikos, A.G. (2017). Extrusion-based 3D printing of poly(propylene fumarate) scaffolds with hydroxyapatite gradients.

J. Biomater. Sci. Polym. Ed. *28*, 532–554. https://doi.org/10.1080/09205063.2017.1286184.

Tripathi, A., Saravanan, S., Pattnaik, S., Moorthi, A., Partridge, N.C., and Selvamurugan, N. (2012). Bio-composite scaffolds containing chitosan/nano-hydroxyapatite/nano-copper-zinc for bone tissue engineering. Int. J. Biol. Macromol *50*, 294–299. https://doi.org/10.1016/j.ijbiomac.2011.11.013.

Ulag, S., Kalkandelen, C., Oktar, F., Uzun, M., Sahin, Y., Karademir, B., Arslan, S., Ozbolat, I., Mahirogullari, M., and Gunduz, O. (2019). 3D printing artificial blood vessel constructs using PCL/Chitosan/Hydrogel biocomposites. Chemistryselect *4*, 2387–2391. https://doi.org/10.1002/slct.201803740.

Vernengo, A., Grad, S., Eglin, D., Alini, M., and Li, Z. (2020). Bioprinting tissue analogues with decellularized extracellular matrix bioink for regeneration and tissue models of cartilage and intervertebral discs. Adv. Funct. Mater *30*, 1909044. https://doi.org/10.1002/adfm.201909044.

Viola, M., Piluso, S., Groll, J., Vermonden, T., Malda, J., and Castilho, M. (2021). The importance of interfaces in multi-material biofabricated tissue structures. Adv. Healthc. Mater. *10*, 2101021. https://doi.org/10.1002/adhm.202101021.

Visser, J., Melchels, F., Jeon, J., van Bussel, E., Kimpton, L., Byrne, H., Dhert, W., Dalton, P., Hutmacher, D., and Malda, J. (2015a). Reinforcement of hydrogels using three-dimensionally printed microfibres. Nat. Commun *6*, 6933. https://doi.org/10.1038/ncomms7933.

Visser, J., Melchels, F.P.W., Jeon, J.E., van Bussel, E.M., Kimpton, L.S., Byrne, H.M., Dhert, W.J.A., Dalton, P.D., Hutmacher, D.W., and Malda, J. (2015b). Reinforcement of hydrogels using three-dimensionally printed microfibres. Nat. Commun *6*, 6933. https://doi.org/10.1038/ncomms7933.

Visser, J., Peters, B., Burger, T., Boomstra, J., Dhert, W., Melchels, F., and Malda, J. (2013). Biofabrication of multi-material anatomically shaped tissue constructs. Biofabrication *5*, 035007. https://doi.org/10.1088/1758-5082/5/3/035007.

Wang, D., Ker, D.F.E., Ng, K.W., Li, K., Gharaibeh, B., Safran, M., Cheung, E., Campbell, P., Weiss, L., and Yang, Y.Z.P. (2021). Combinatorial mechanical gradation and growth factor biopatterning strategy for spatially controlled bone-tendon-like cell differentiation and tissue formation. Npg Asia Mater *13*, 26. https://doi.org/10.1038/s41427-021-00294-z.

Wang, X., Yan, Y., Pan, Y., Xiong, Z., Liu, H., Cheng, B., Liu, F., Lin, F., Wu, R., Zhang, R., and Lu, Q. (2006). Generation of three-dimensional hepatocyte/gelatin structures with rapid prototyping system. Tissue Eng. *12*, 83–90. https://doi.org/10.1089/ten.2006.12.83.

Wang, Z.J., Abdulla, R., Parker, B., Samanipour, R., Ghosh, S., and Kim, K. (2015). A simple and high-resolution stereolithography-based 3D bioprinting system using visible light crosslinkable bioinks. Biofabrication *7*, 045009. https://doi.org/10.1088/1758-5090/7/4/045009.

Warnke, P., Seitz, H., Warnke, F., Becker, S., Sivananthan, S., Sherry, E., Liu, Q., Wiltfang, J., and Douglas, T. (2010). Ceramic scaffolds produced by computer-assisted 3D printing and sintering: characterization and biocompatibility investigations. J. Biomed. Mater. Res. Part B-Applied Biomater. *93B*, 212–217. https://doi.org/10.1002/jbm.b.31577.

Welsh, R.P., Pilliar, R.M., and Macnab, I. (1971). Surgical implants. The role of surface porosity in fixation to bone and acrylic. J. Bone Joint Surg Am *53*, 963–977.

Wen, P., Voshage, M., Jauer, L., Chen, Y., Qin, Y., Poprawe, R., and Schleifenbaum, J. (2018). Laser additive manufacturing of Zn metal parts for biodegradable applications: processing, formation quality and mechanical properties. Mater. Des. *155*, 36–45. https://doi.org/10.1016/j.matdes.2018.05.057.

Wenz, A., Borchers, K., Tovar, G., and Kluger, P. (2017). Bone matrix production in hydroxyapatite-modified hydrogels suitable for bone bioprinting. Biofabrication *9*, 044103. https://doi.org/10.1088/1758-5090/aa91ec.

Williams, J.M., Adewunmi, A., Schek, R.M., Flanagan, C.L., Krebsbach, P.H., Feinberg, S.E., Hollister, S.J., and Das, S. (2005). Bone tissue engineering using polycaprolactone scaffolds fabricated via selective laser sintering. Biomaterials *26*, 4817–4827. https://doi.org/10.1016/j.biomaterials.2004.11.057.

Wilson, W., and Boland, T. (2003). Cell and organ printing 1: protein and cell printers. Anatomical Rec. A-Discoveries Mol. Cell Evol. Biol. *272A*, 491–496. https://doi.org/10.1002/ar.a.10057.

Woodard, J., Hilldore, A., Lan, S., Park, C., Morgan, A., Eurell, J., Clark, S., Wheeler, M., Jamison, R., and Johnson, A. (2007). The mechanical properties and osteoconductivity of hydroxyapatite bone scaffolds with multi-scale porosity. Biomaterials *28*, 45–54. https://doi.org/10.1016/j.biomaterials.2006.08.021.

Wu, C., Luo, Y., Cuniberti, G., Xiao, Y., and Gelinsky, M. (2011). Three-dimensional printing of hierarchical and tough mesoporous bioactive glass scaffolds with a controllable pore architecture, excellent mechanical strength and mineralization ability. Acta Biomater. *7*, 2644–2650. https://doi.org/10.1016/j.actbio.2011.03.009.

Wu, D., Spanou, A., Diez-Escudero, A., and Persson, C. (2020). 3D-printed PLA/HA composite structures as synthetic trabecular bone: a feasibility study using fused deposition modeling. J. Mech. Behav. Biomed *103*, 103608. https://doi.org/10.1016/j.jmbbm.2019.103608.

Wu, W., Geng, P., Li, G., Zhao, D., Zhang, H., and Zhao, J. (2015). Influence of layer thickness and raster angle on the mechanical properties of 3D-printed PEEK and a comparative mechanical study between PEEK and ABS. Materials *8*, 5834–5846. https://doi.org/10.3390/ma8095271.

Wu, Y.H.A., Chiu, Y.C., Lin, Y.H., Ho, C.C., Shie, M.Y., and Chen, Y.W. (2019). 3D-Printed bioactive calcium silicate/poly-epsilon-caprolactone bioscaffolds modified with biomimetic extracellular matrices for bone regeneration. Int. J. Mol. Sci *20*, 942. https://doi.org/10.3390/ijms20040942.

Wust, S., Godla, M., Muller, R., and Hofmann, S. (2014). Tunable hydrogel composite with two-step processing in combination with innovative hardware upgrade for cell-based three-dimensional bioprinting. Acta Biomater. *10*, 630–640. https://doi.org/10.1016/j.actbio.2013.10.016.

Xu, C., Chai, W., Huang, Y., and Markwald, R.R. (2012a). Scaffold-free inkjet printing of three-dimensional zigzag cellular tubes. Biotechnol. Bioeng. *109*, 3152–3160. https://doi.org/10.1002/bit.24591.

Xu, F., Inci, F., Mullick, O., Gurkan, U., Sung, Y., Kavaz, D., Li, B., Denkbas, E., and Demirci, U. (2012b). Release of magnetic nanoparticles from cell-encapsulating biodegradable nanobiomaterials. Acs Nano *6*, 6640–6649. https://doi.org/10.1021/nn300902w.

Xu, T., Binder, K., Albanna, M., Dice, D., Zhao, W., Yoo, J., and Atala, A. (2013). Hybrid printing of mechanically and biologically improved constructs for cartilage tissue engineering applications. Biofabrication *5*, 015001. https://doi.org/10.1088/1758-5082/5/1/015001.

Xu, Z., Wang, N., Liu, P., Sun, Y., Wang, Y., Fei, F., Zhang, S., Zheng, J., and Han, B. (2019). Poly(Dopamine) coating on 3D-printed poly-lactic-Co-glycolic acid/β-tricalcium phosphate scaffolds for bone tissue engineering. Molecules *24*. https://doi.org/10.3390/molecules24234397.

Yang, C., Tian, X., Li, D., Cao, Y., Zhao, F., and Shi, C. (2017). Influence of thermal processing conditions in 3D printing on the crystallinity and mechanical properties of PEEK material. J. Mater. Process. Technology *248*, 1–7. https://doi.org/10.1016/j.jmatprotec.2017.04.027.

Yang, Y., Yang, S., Wang, Y., Yu, Z., Ao, H., Zhang, H., Qin, L., Guillaume, O., Eglin, D., Richards, R., and Tang, T. (2016a). Anti-infective efficacy, cytocompatibility and biocompatibility of a 3D-printed osteoconductive composite scaffold functionalized with quaternized chitosan. Acta Biomater. *46*, 112–128. https://doi.org/10.1016/j.actbio.2016.09.035.

Yang, Y., Yang, S., Wang, Y., Yu, Z., Ao, H., Zhang, H., Qin, L., Guillaume, O., Eglin, D., Richards, R.G., and Tang, T. (2016b). Anti-infective efficacy, cytocompatibility and biocompatibility of a 3D-printed osteoconductive composite scaffold functionalized with quaternized chitosan. Acta Biomater. *46*, 112–128. https://doi.org/10.1016/j.actbio.2016.09.035.

Ye, K., Felimban, R., Traianedes, K., Moulton, S.E., Wallace, G.G., Chung, J., Quigley, A., Choong, P.F., and Myers, D.E. (2014). Chondrogenesis of infrapatellar fat pad derived adipose stem cells in 3D printed chitosan scaffold. PLoS One *9*, e99410. https://doi.org/10.1371/journal.pone.0099410.

Yelin, E., Weinstein, S., and King, T. (2016). The burden of musculoskeletal diseases in the United States. Semin. Arthritis Rheum. *46*, 259–260. https://doi.org/10.1016/j.semarthrit.2016.07.013.

Yen, H., Tseng, C., Hsu, S., and Tsai, C. (2009). Evaluation of chondrocyte growth in the highly porous scaffolds made by fused deposition manufacturing (FDM) filled with type II collagen. Biomed. Microdevices *11*, 615–624. https://doi.org/10.1007/s10544-008-9271-7.

Yeo, T., Ko, Y., Kim, E., Kwon, O., Chung, H., and Kwon, O. (2021). Promoting bone regeneration by 3D-printed poly(glycolic acid)/hydroxyapatite composite scaffolds. J. Ind. Eng. Chem. *94*, 343–351. https://doi.org/10.1016/j.jiec.2020.11.004.

Yeong, W.Y., Sudarmadji, N., Yu, H.Y., Chua, C.K., Leong, K.F., Venkatraman, S.S., Boey, Y.C.F., and Tan, L.P. (2010). Porous polycaprolactone scaffold for cardiac tissue engineering fabricated by selective laser sintering. Acta Biomater. *6*, 2028–2034. https://doi.org/10.1016/j.actbio.2009.12.033.

Ying, Z.M., Lin, T., and Yan, S.G. (2014). Arthroscopic single-row versus double-row technique for repairing rotator cuff tears: a systematic review and meta-analysis. Orthop. Surg. *6*, 300–312. https://doi.org/10.1111/os.12139.

You, F., Chen, X., Cooper, D., Chang, T., and Eames, B. (2019). Homogeneous hydroxyapatite/alginate composite hydrogel promotes calcified cartilage matrix deposition with potential for three-dimensional bioprinting. Biofabrication *11*, 015015. https://doi.org/10.1088/1758-5090/aaf44a.

Yue, K., Trujillo-de Santiago, G., Alvarez, M., Tamayol, A., Annabi, N., and Khademhosseini, A. (2015). Synthesis, properties, and biomedical applications of gelatin methacryloyl (GelMA) hydrogels. Biomaterials *73*, 254–271. https://doi.org/10.1016/j.biomaterials.2015.08.045.

Yusa, K., Yamamoto, O., Fukuda, M., Koyota, S., Koizumi, Y., and Sugiyama, T. (2011). In vitro prominent bone regeneration by release zinc ion from Zn-modified implant. Biochem. Biophysical Res. Commun. *412*, 273–278. https://doi.org/10.1016/j.bbrc.2011.07.082.

Zafar, M., Zhu, D., and Zhang, Z. (2019). 3D printing of bioceramics for bone tissue engineering. Materials *12*, 3361. https://doi.org/10.3390/ma12203361.

Zanjanijam, A., Major, I., Lyons, J., Lafont, U., and Devine, D. (2020). Fused filament fabrication of PEEK: a review of process-structure-property relationships. Polymers *12*, 1665. https://doi.org/10.3390/polym12081665.

Zhang, J., Allardyce, B., Rajkhowa, R., Zhao, Y., Dilley, R., Redmond, S., Wang, X., and Liu, X. (2018). 3D printing of silk particle-reinforced chitosan hydrogel structures and their properties. Acs Biomater. Sci. Eng. *4*, 3036–3046. https://doi.org/10.1021/acsbiomaterials.8b00804.

Zhang, X., Wang, J., and Liu, T. (2021a). 3D printing of polycaprolactone-based composites with diversely tunable mechanical gradients via multi-material fused deposition modeling. Composites Commun. *23*, 100600. https://doi.org/10.1016/j.coco.2020.100600.

Zhang, Y., Yu, Y., Chen, H., and Ozbolat, I. (2013). Characterization of printable cellular micro-fluidic channels for tissue engineering. Biofabrication *5*, 025004. https://doi.org/10.1088/1758-5082/5/2/025004.

Zhang, Y.J., Lei, T.Y., Tang, C.Q., Chen, Y.W., Liao, Y.G., Ju, W., Zhang, H., Zhou, B., Liang, R.J., Zhang, T., et al. (2021b). 3D printing of chemical-empowered tendon stem/progenitor cells for functional tissue repair. Biomaterials *271*, 120722. https://doi.org/10.1016/j.biomaterials.2021.120722.

Zhang, Z., He, F., Wang, B., Zhao, Y., Wei, Z., Zhang, H., and Sang, L. (2021c). Biodegradable PGA/PBAT blends for 3D printing: material performance and periodic minimal surface structures. Polymers *13*, 3757. https://doi.org/10.3390/polym13213757.

Zhao, C., Liu, W., Xu, Z., Li, J., Huang, T., Lu, Y., Huang, H., and Lin, J. (2020a). Chitosan ducts fabricated by extrusion-based 3D printing for soft-tissue engineering. Carbohydr. Polym *236*, 116058. https://doi.org/10.1016/j.carbpol.2020.116058.

Zhao, F., Cheng, J., Sun, M., Yu, H., Wu, N., Li, Z., Zhang, J., Li, Q., Yang, P., Liu, Q., et al. (2020b). Digestion degree is a key factor to regulate the printability of pure tendon decellularized extracellular matrix bio-ink in extrusion-based 3D cell printing. Biofabrication *12*, 045011. https://doi.org/10.1088/1758-5090/aba411.

Zhao, F., Cheng, J., Zhang, J., Yu, H., Dai, W., Yan, W., Sun, M., Ding, G., Li, Q., Meng, Q., et al. (2021). Comparison of three different acidic solutions in tendon decellularized extracellular matrix bio-ink fabrication for 3D cell printing. Acta Biomater. *131*, 262–275. https://doi.org/10.1016/j.actbio.2021.06.026.

Zhao, Z., Li, J., Wei, Y., and Yu, T. (2022). Design and properties of graded polyamide12/hydroxyapatite scaffolds based on primitive lattices using selective laser sintering. J. Mech. Behav. Biomed. Mater. *126*, 105052. https://doi.org/10.1016/j.jmbbm.2021.105052.

Zheng, Y.H., Han, Q., Li, D.D., Sheng, F., Song, Z.M., and Wang, J.C. (2021). Promotion of tendon growth into implant through pore-size design of a Ti-6Al-4 V porous scaffold prepared by 3D printing. Mater. Des *197*, 109219. https://doi.org/10.1016/j.matdes.2020.109219.

Zhou, X., Zhu, W., Nowicki, M., Miao, S., Cui, H., Holmes, B., Glazer, R., and Zhang, L. (2016). 3D ioprinting a cell-laden bone matrix for breast cancer metastasis study. Acs Appl. Mater. Inter. *8*, 30017–30026. https://doi.org/10.1021/acsami.6b10673.

Zhu, M., Wang, Y., Ferracci, G., Zheng, J., Cho, N.J., and Lee, B.H. (2019). Gelatin methacryloyl and its hydrogels with an exceptional degree of controllability and batch-to-batch consistency. Sci. Rep. *9*, 6863. https://doi.org/10.1038/s41598-019-42186-x.

Zimmerling, A., Yazdanpanah, Z., Cooper, D.M.L., Johnston, J.D., and Chen, X. (2021). 3D printing PCL/nHA bone scaffolds: exploring the influence of material synthesis techniques. Biomater. Res. *21*, 1–12.

Zuo, Y., Xiao, W., Chen, X., Tang, Y., Luo, H., and Fan, H. (2012). Bottom-up approach to build osteon-like structure by cell-laden photocrosslinkable hydrogel. Chem. Commun. *48*, 3170–3172. https://doi.org/10.1039/c2cc16744a.

Zysset, P.K., Guo, X.E., Hoffler, C.E., Moore, K.E., and Goldstein, S.A. (1999). Elastic modulus and hardness of cortical and trabecular bone lamellae measured by nanoindentation in the human femur. J. Biomech. *32*, 1005–1012. https://doi.org/10.1016/s0021-9290(99)00111-6.